

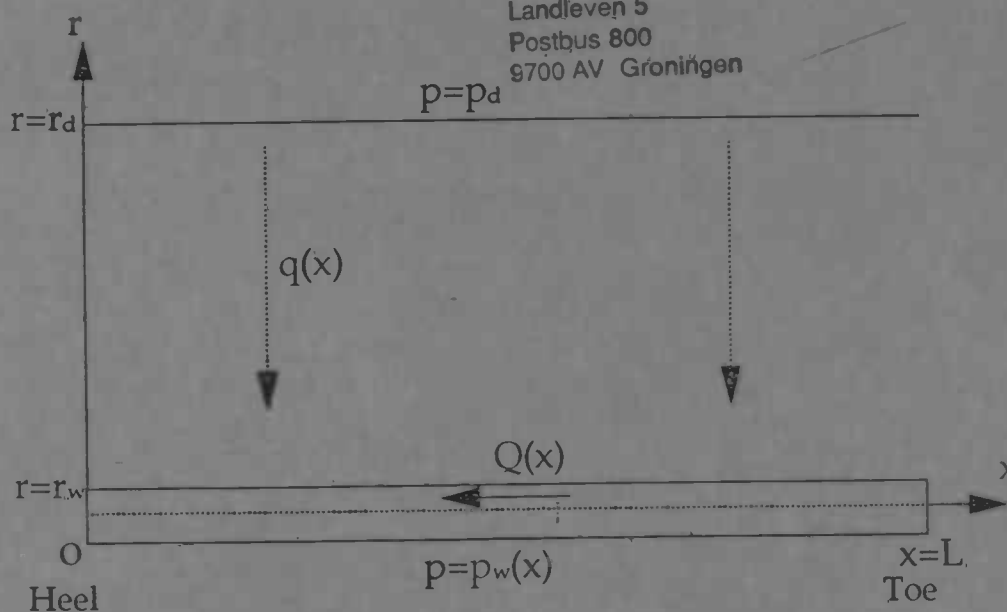
WORDT  
NIET UITGELEEND



# Modelling of Horizontal Wells

H. Eppinga

Rijksuniversiteit Groningen  
Bibliotheek Informatica / Rekencentrum  
Landleven 5  
Postbus 800  
9700 AV Groningen



Rijksuniversiteit Groningen  
Bibliotheek  
Wiskunde / Informatica / Rekencentrum  
Landleven 5  
Postbus 800  
9700 AV Groningen

Department of  
Mathematics

**RUG**



Master's Thesis

---

# Modelling of Horizontal Wells

H. Eppinga

---

Rijksuniversiteit Groningen  
**Bibliotheek Informatica / Rekencentrum**  
Landleven 5  
Postbus 800  
9700 AV Groningen

Rijksuniversiteit Groningen  
Vakgroep Wiskunde  
Postbus 800  
9700 AV Groningen

December 1996

To my family and old friends,  
who I have not seen for a while  
and  
to new friends,  
who I want to see again.

# Preface

This graduate research for the university of Groningen, the Netherlands, was done at the research centre of Norsk Hydro at Porsgrunn, Norway under supervision of dr R. Schulkes. Before starting with this study I did not know anything about oil production and horizontal wells. After reading about the subject I discovered that the whole oil production process is quite sophisticated, complex and interesting. The fact that mathematical models are used in combination with experimental data for the prediction of the production characteristics of a horizontal well was very interesting for me. Therefore, I enjoyed the study and hope to do more research on this topic.

The author is a student at the university of Groningen at the Mathematical Department with graduate direction Technical Mechanics; graduate teacher prof. dr A.E.P Veldman. The graduate direction can be seen as a Applied Mathematics with a special attention to Computational Fluid Dynamics and results in an engineer degree, i.e. Master of Science, (april 1997).

Norsk Hydro a.s.  
Research Centre Porsgrunn  
P.O. box 2560  
N-3901 Porsgrunn  
Norway

Rijksuniversiteit Groningen  
Department of Mathematics  
P.O. box 800  
9700 AV Groningen  
The Netherlands.

Hendrik Eppinga  
Jac. Boomsmastr. 37  
8565 GG Sondel(Frl.)  
The Netherlands  
tel: 0514-602784  
e-mail : csg540@wing.rug.nl

# Contents

<b>1</b>	<b>Introduction to horizontal wells</b>	<b>2</b>
1.1	Horizontal wells . . . . .	2
1.2	Models of horizontal wells . . . . .	5
1.3	Outline of this report . . . . .	6
<b>2</b>	<b>The model</b>	<b>8</b>
2.1	Introduction . . . . .	8
2.2	The model equations . . . . .	9
2.3	Model properties . . . . .	12
<b>3</b>	<b>Numerical solution of the model</b>	<b>16</b>
3.1	Linearisation . . . . .	16
3.2	Discretisation . . . . .	17
<b>4</b>	<b>Results</b>	<b>21</b>
4.1	Numerical analysis and results . . . . .	21
4.2	Model analysis . . . . .	23
4.2.1	Introduction . . . . .	23
4.2.2	Analysis of the drawdown . . . . .	23
4.2.3	Analysis of the other parameters . . . . .	25
4.3	A comparison with other models. . . . .	29
<b>5</b>	<b>An extended model</b>	<b>31</b>
5.1	Introduction . . . . .	31
5.2	Model equations . . . . .	31
5.3	Numerical solution of the model . . . . .	33
5.4	Model properties . . . . .	34
<b>6</b>	<b>Analysis of the extended model</b>	<b>36</b>
6.1	Introduction . . . . .	36
6.2	Analysis of the influence of ICD's . . . . .	37
<b>7</b>	<b>Discussions, extensions and conclusions</b>	<b>40</b>
7.1	Discussion about the assumptions . . . . .	40
7.2	Model extensions . . . . .	41

7.3 Conclusions . . . . .	42
<b>A The reservoir</b>	<b>46</b>
<b>B The pressure drop in a pipe with radial inflow</b>	<b>49</b>
<b>C Stability</b>	<b>51</b>
<b>Supplements</b>	<b>54</b>
I Norsk Hydro . . . . .	54
II Experimental work . . . . .	55

## Abstract

The results of a study on the modelling aspects of horizontal wells are described in this report. The derived 1D-model is based on both experimental and theoretical work and contains therefore several extensions compared to some other existing models. The obtained model equations are solved in such a way that the developed code is efficient and in particular, offers the possibility to give in all the model parameters including the well length. The code is therefore used as a tool for an extended, and described, analysis on the influence of the model parameters on the production characteristics. This analysis could give more insight in horizontal wells which can lead to better modelling work. The analysis also includes an investigation on the use of ICDs. Since more extensions are possible, recommendations for the future are described and discussed.

# Chapter 1

## Introduction to horizontal wells

### 1.1 Horizontal wells

Oil is produced from oil containing reservoirs which consist mostly of geological sand layers. The reservoirs can have different shapes, generally they can be divided into three types : 'balloon-shaped', 'lens shaped' and layered reservoirs. See Figure 1.1.1.

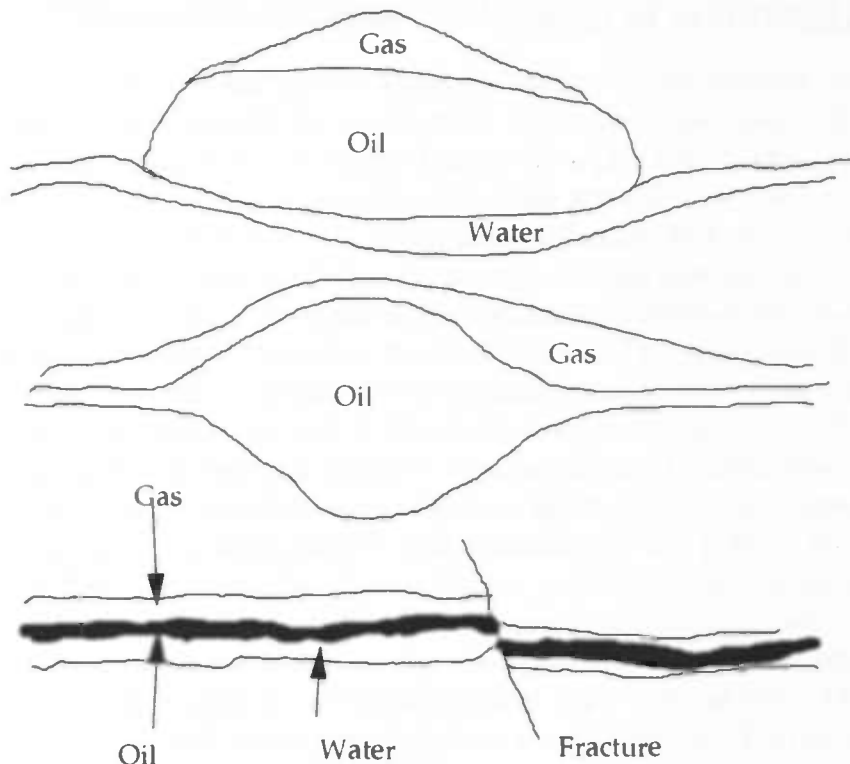


**Figure 1.1.1:** A 'balloon shaped' a 'lens shaped' and a layered reservoir.

Most of the balloon-shaped fields are already in production or emptied because it is relatively easy and cheap to produce oil from these fields. The lens shaped reservoirs have a thick centre region which may be relatively easy to empty as well. However, the

thin edges of these fields contain oil which may be hard to recover. Some of these fields have a centre that has been emptied a long time ago, while the edges have been drained only recently or still have to be drained. The layered reservoirs are generally long and relatively thin; the oil layers can have a thickness of only a few meters whereas the length of the reservoirs can be up to a few kilometres. This shape makes it more complicated to produce the oil in an economically way from these type of fields. Significant amounts of the currently known oil reserves can be found in reservoirs with a layered shape. In order to drain these fields, a lot of horizontal wells will be drilled in the future.

Horizontal wells are the only economically method for draining the thin and long reservoirs. The required technical knowledge for horizontal drilling has become available the last ten to fifteen years. In addition to offering the possibility for draining the thin and long reservoirs, some old fields become economically interesting again. For example, horizontal wells make it possible to drain the thin edges of the 'lens shaped' reservoirs.

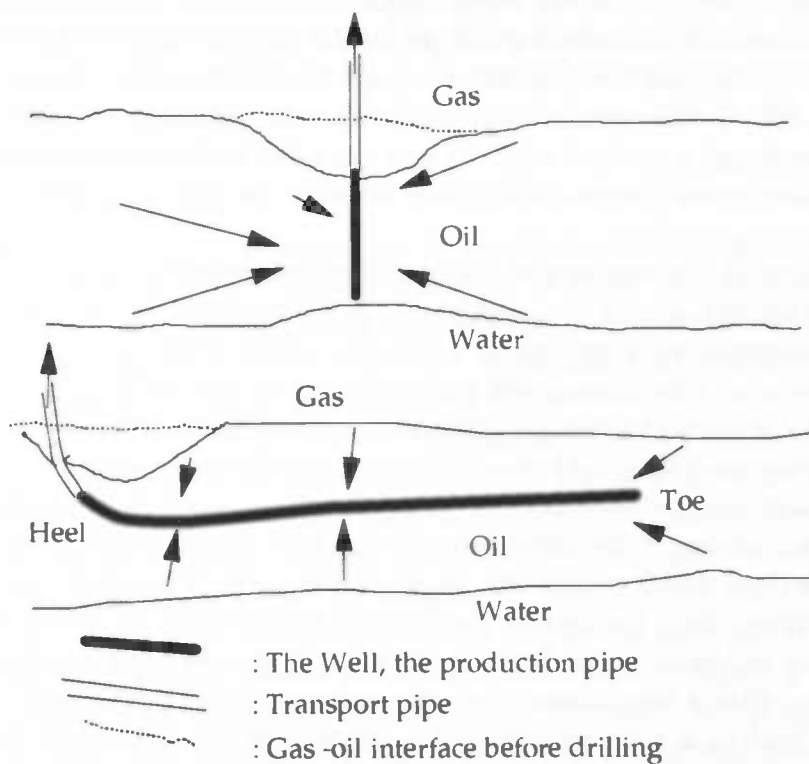


**Figure 1.1.2:** A layered reservoir with a vertical and horizontal well.

Figure 1.1.2 shows a horizontal and a vertical well in a layered reservoir, the names of some parts of the well are also shown in this figure. As one can see, a horizontal well consists of a horizontal section and is connected with a vertical section. The vertical part is meant for the transport of the oil upwards and consists therefore of a smooth pipe, whereas the horizontal section is meant for the production and consists therefore of a perforated pipe, the production pipe. The start of the perforated section is called the heel of the well and the end of the production pipe is called the toe of the well. The section between the heel and the toe is referred to as the well. It can also be seen in the figure

that a vertical well has a very short production part; approximately equal to the thickness of the oil layer.

Horizontal wells have a lot of advantages compared to vertical wells, especially when the oil is produced from a long and thin reservoir. The important advantages, i.e. the advantages that are caused by the larger contact area, will be mentioned in this report. The contact area of a well is defined as the area of the well which is in contact with the oil. A vertical well has only a contact area over a length of at most the thickness of the oil layer, whereas a horizontal well can be in contact with the oil along its total horizontal section. The larger contact area makes a horizontal well economically interesting for the production of oil. In addition, the inflow occurs along the whole contact area, which means that, in case of a horizontal well, the oil is drained from the reservoir relatively even. The even inflow for a horizontal well is a big advantage, in particular in thin reservoirs which are bounded above by a gas layer and bounded below by a water layer. The reason is that the oil production can reduce significantly when a breakthrough of gas or water occurs. An eventual breakthrough of gas and/or should therefore be delayed as long as possible. This can be achieved by using a horizontal well rather than a vertical one, see also Figure 1.1.2. The figure shows the movement of the oil and the oil-gas interface towards a horizontal and a vertical well. As one can see a horizontal well can give a more slow and even movement of the gas-oil interface towards the well compared to vertical well.

So far, only the major advantages of horizontal wells were mentioned, but also the most important disadvantages should be mentioned. A detailed description of the particular problems with horizontal wells is given by Tehrani *et al* [TP,1993]. The problems that can show up when one uses a horizontal well rather than a vertical well are mostly caused by the long horizontal section of the well. Since the production at a certain point of the well depends on the pressure difference between the well and the drainage area in the reservoir at that certain point, i.e. the drawdown at that point, a decrease of the drawdown towards the toe will give a decrease of the inflow towards the toe. The drawdown decrease because of to the pressure drop which occurs due to several reasons. The most important reason for the pressure drop along the well is the friction experienced by the flow in the well. The pressure drop in the well can become even larger due to sand production and due to multiphase flow after a breakthrough of gas or water. Sand is produced together with the oil and may lead to a sand particle sedimentation at the bottom of the pipe. This gives a smaller flow area and therefore a higher pressure drop. Multiphase flow may increase the effective viscosity of the well fluid and gives an additional contribution to the pressure drop. The problems due to the sand production and multiphase flow do not occur so strongly in the cases of the oil production via a vertical well. The pressure loss can make a horizontal well less interesting than a vertical well. Furthermore, it should also be mentioned that a horizontal well can intersect several reservoir fractures. These fractures can have a bad influence on the production performance, in particular if the fractures intersect gas or water in the reservoir.

## 1.2 Models of horizontal wells

In general, models of horizontal wells are made for three purposes. Models may be used for planning the well, i.e. give insight in the optimal well length, optimal drawdown etc. Models can also be used for a prediction of the problems that can occur. Good models may be able to predict the place and moment of a possible gas or water breakthrough. Finally, models can be used to explain measurements in order to get insight in the reservoir properties. A lot of models already have been made for horizontal wells. An overview of these models is given below, together with their limitations and benefits. The single phase models are listed first.

The first models made use of potential theory. These models assume an incompressible fluid and negligible pressure drop in the well compared to the one in the reservoir. A combination of the equation of Darcy with the continuity equation leads to a potential equation. The solution can be estimated by using the analytical solution obtained after a conversion from the 3D problem into a more easy 2D potential equation. This results in a linear equation for the drawdown,  $\mathcal{D}$  [Pa], the total production rate,  $Q$  [m<sup>3</sup>/s] and the productivity index, PI [m<sup>3</sup>/s/Pa]:

$$Q = PI \cdot \mathcal{D}.$$

The PI is a measure of the productivity of the reservoir and can therefore be used to compare different wells. The biggest limitation of these models that the drawdown is assumed to be constant while in reality the pressure changes significantly along long wells. These models can only be used for very short wells. More information on these potential theory-models can be found in the papers of Giger *et al* [GR,1984], Joshi [SJ,1987] & [SJ,1988] and Renard *et al* [RD,1990]. A derivation of the PI can be found in [SJ,1987]

Simulations with the developed code show that the total pressure loss along the well can be up to half the value of the drawdown at the heel. This means that the pressure drop in the well should be included in order to make the model more accurate. The pressure drop in the well can be calculated by using a PI per meter,  $J_s$  [m<sup>3</sup>/day/bar/m], rather than the PI for a total well. The specific PI can be used to calculate the inflow per meter using the drawdown at that certain point. One of the first attempting to model this, was Dikken [BD,1990]. The result is a relative simple 1D-model, which takes in account the friction in the well. The results show that the friction in the well can not be ignored, it gives an increase of the inflow towards the heel and has therefore a significant influence on the production performance of a horizontal well. Another model, using the same assumptions as in Dikken's model, is the model of Holte [SH,1993], of which derivation of the specific PI is included in his paper. The advantage of the models of Holte and Dikken is the inclusion of important physics in the model. The biggest limitation however is that the reservoir is only taken in account via one simple parameter, the specific PI. This results in a reservoir flow with no horizontal component. However, the horizontal flow in a reservoir is often negligible in large section of the well, in particular when the well is long. Therefore, the two mentioned models can be seen as a relative simple tool, which can be used to gain more insight in the complexity of horizontal wells.

A totally different approach is used by Landman *et al* [LG,1991] and Maret *et al*

[ML,1993]. They treat the well as a collection of point sinks. The pressure in the reservoir is governed by Darcy's equation which gives the inflow in each perforation. The pressure in the well is calculated by including pressure losses. These models can be used to analyse the influence of a non uniform perforation density along the well.

The inclusion of pressure drop in the well should give better results, but it is more complicated to take account of the size of the reservoir and the effect of the difference in horizontal and vertical permeability, anisotropy. Ozkan *et al* [OS,1992] developed an instationar, 3D single phase model which includes the mentioned physical aspects of the well.

In order to give more accurate predictions a 3D multi phase model can be used. Present models achieve this by coupling a reservoir and a well simulator. Examples of this approach are given by Korady *et al* [KR,1991], Brekke *et al* [BJ,1993] and Alvestad *et al* [AH,1994]. Korady *et al* use a linear relation between the inflow and the drawdown, which gives a 3D convection-diffusion equation. Brekke *et al* and Alvestad *et al* couple a well-simulator with a reservoir-simulator, which results in rather complicated models.

The model in this report is based on the model of Dikken. In addition some extensions in several directions are investigated. First, the acceleration of the inflow along the well is investigated. After a calculation it is found that it has no a significant contribution on the pressure drop. A correction on the friction, due to the perturbation by the inflow, does not have to be included in the calculation of the pressure drop either. Another extension concerns the friction losses through the pipe wall, which result in a non-linear inflow-drawdown relation. Although the friction is negligible for a normal production pipe, it has to be included in some special cases. The model equations are solved by using a quadratic iteration scheme in combination with second order finite difference methods. The solution method used by Dikken is not easy to use. The model is treated like an initial value problem. This means that the well length can not be used as an input parameter and has to be obtained by trial and error. The solution method described in this report offers the possibility to put in all the required model parameters individually and also the possibility for prescribing the boundary conditions at both the heel and the toe.

The goal of this study is to develop more accurate models, which can be used to predict the production characteristics of horizontal wells in a steady state. The developed code, which is very flexible, can be used to perform simulations in order to increase our understanding of important physical aspects of horizontal wells and in order to be able to explain measurements.

### 1.3 Outline of this report

The governing equations for the first model, that will be presented in this report, are derived in chapter 2. The linearisation method, which leads to a quadratically convergent iteration scheme, is presented in section 3.1. The last part of the solution method is the use of the finite difference method, this is done in section 3.2. The actual goal of this study is to

gain more insight in the production characteristics of a horizontal well. In order to gain this insight, an extended analysis of the influence of all the model parameters is given in chapter 4. Chapters 6 and 7 are dedicated to an interesting extension of the model and the application of this extension. Since the two developed models contain simplifications and limitations, a discussion on the assumptions and the possible extensions is given in the last chapter of the report. Finally, the appendices contain some more detailed information about the reservoir, the friction in the pipe, the discretisation methods and the stability of the developed code.

## Chapter 2

### The model

#### 2.1 Introduction

The models of B.J. Dikken and S.T. Holte are used to derive an improved model for the steady state flow in an horizontal well. First, some assumptions are made. They are necessary for the derivation of the governing equations. A discussion on these assumptions can be found in section 7.1.

Assumptions :

- 1 : The well contains no differences in height over its total length.
- 2 : Flow inside the well is single phase and turbulent.
- 3 : The production line is perforated with a given perforation density.
- 4 : The properties of the well and the reservoir do not change with the time, i.e. a steady state exists.
- 5 : The pressure in the well depends only on the  $x$ -coordinate in the well.
- 6 : The inflow depends linearly on the pressure difference between the well and the reservoir.
- 7 : The reservoir has constant properties along the well.
- 8 : There exists a constant pressure in the reservoir at a constant distance from the well.

The model-equations for the calculation of the pressure-drop in a horizontal well will be derived in the next section. Therefore, some of the variables and terms will be shown in figure Figure 2.1.1. As one can see, the positive  $x$ -direction is chosen from the heel towards the toe. The figure shows furthermore that the main volume flow,  $Q(x)$  runs from the toe towards the heel. The assumed constant pressure boundary in the reservoir is also shown in the figure. At distance  $r = r_d$  of the well there is a boundary with a constant pressure  $p_d$ . This pressure can be seen as a reference pressure.

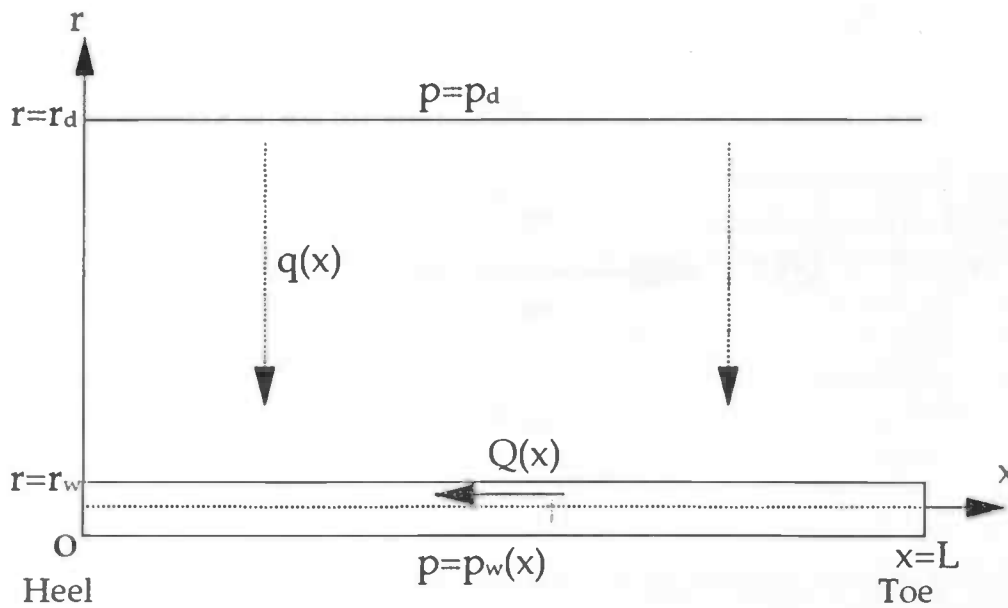


Figure 2.1.1 : The well and some of its variables and quantities.

## 2.2 The model equations

The model equations can be divided into three parts. One part relates the inflow with the pressure difference between the well and the reservoir. A mass balance is used to describe the relation between the inflow and the main flow. The last part is the pressure drop in the well due to several contributions.

It is assumed that a linear relation between the pressure difference and the inflow exists, i.e.

$$q(x) = J_s [p_d - p_w(x)], \quad (2.1)$$

with

$q(x)$  = the inflow rate per meter, [ $\text{m}^3/\text{s}/\text{m}$ ],

$J_s$  = the specific productivity index, relates the inflow and the drawdown, [ $\text{Sm}^3/\text{s}/\text{Pa}/\text{m}$ ],

$p_d$  = the constant pressure in the reservoir at a constant distance from the well, [Pa]

$p_w(x)$  = the pressure in the well [Pa].

The details about the inflow-pressure difference relation and a derivation of the value of the specific PI can be found in Appendix A. Furthermore, the difference in pressure between the reservoir and the well is referred to as the drawdown.

If the production rate is given by  $Q(x)$ , then a mass balance,  $Q(x + dx) + dx \cdot q(x) = Q(x)$ , can be used to relate the inflow and the main flow. This results in

$$q(x) = -\frac{dQ}{dx}(x). \quad (2.2)$$

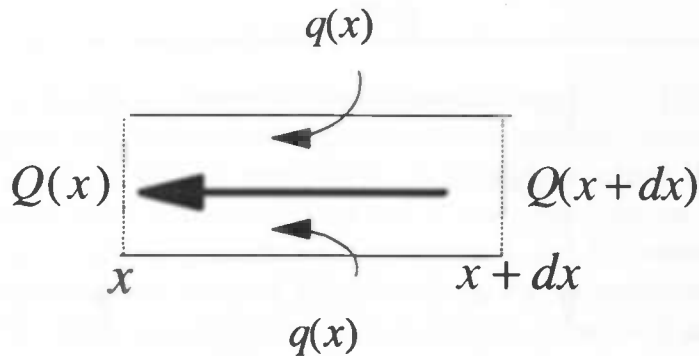


Figure 2.2.1: A visualisation of the used mass balance.

The pressure-loss in the well is due to two effects: friction and acceleration. Therefore, the pressure gradient can be written as

$$\frac{dp_w}{dx}(x) = \frac{dp_f}{dx}(x) + \frac{dp_a}{dx}(x) \quad (2.3)$$

Friction is the major reason for pressure loss. The pressure gradient due to friction in a pipe *without* radial inflow and a fully developed turbulent flow is commonly written as:

$$\frac{dp_f}{dx} = \frac{\rho}{2d} f(Q(x)) \frac{Q^2}{A^2}, \quad (2.4)$$

with

- $\rho$  = the density of the flow,
- $d$  = the diameter of the pipe,
- $A$  = the area of the pipe,
- $f(Q)$  = the friction factor.

The flow in the well is assumed to be a fully developed turbulent flow, therefore, equation (2.4) is also used in the equation for the frictional pressure drop in the well. A small correction, however, is required because a well can be seen as a pipe *with* radial inflow. Experiments show that if the inflow is small compared to the main flow, the inflow will give lubrication effect. On the other hand, if the inflow is large compared to the main flow, the inflow can increase the frictional pressure drop. Correcting eq. (2.4) for effects of radial inflow results in:

$$\frac{dp_f}{dx} = \left[ 1 + \lambda d \frac{1}{Q} \frac{dQ}{dx} \right] \frac{\rho}{2d} f(Q(x)) \frac{Q^2}{A^2}, \quad (2.5)$$

where  $\lambda$  is an experimental determined factor, with:  $\lambda \approx 25$ . Experiments on the pressure drop in a well, in particular due to the friction, were done by Utvik *et al* [US,1995] and are described in Appendix B.

It is assumed that the well flow is a complete developed turbulent pipe flow. This assumption is not valid for the whole well but it will be shown in section 7.1 that the

region in which the flow is laminar is a small fraction of the total length of the well. This means that several options are available for the friction factor. The following two options for the friction factor are available in the developed code. The first option is the so-called Blasius equation:

$$f(Q) = 0.3164 Re^{-0.25}, \quad (2.6)$$

where the Reynolds number for a pipe flow is given by

$$Re = \frac{\rho |Q| d}{\mu A^2}. \quad (2.7)$$

This friction factor is based on experiments and can be used for smooth pipes and flows with  $Re < 5 \cdot 10^4$ . For larger Reynolds numbers or rough pipe the Haaland friction factor is a better choice. This friction factor is also based on experiments and is given by:

$$f(Q) = \left[ 1.8 \log \left( \frac{6.9}{Re} + \left[ \frac{\epsilon}{3.7d} \right]^{1.11} \right) \right]^{-2}, \quad (2.8)$$

with  $\epsilon$  a parameter for the roughness of the pipe. The magnitude of the typical roughness on the inner surface of the pipe is measured by  $\epsilon$ , where  $\epsilon \ll d$  has to hold.

As was mentioned acceleration effects also have an influence on the pressure. The inflow does not have any horizontal velocity and the necessary acceleration causes pressure loss. The derivation of the equation is done with a momentum balance. The force,  $dF$ , required for the acceleration of a mass,  $\rho A dx$ , from  $x$  to  $x + dx$  gives the desired equation:

$$dF = \rho A \frac{du}{dt} dx = \frac{\rho A dx}{A} \left[ \frac{dQ}{dx} \frac{dx}{dt} + \frac{dQ}{dt} \right] = 2 \frac{\rho}{A} Q \frac{dQ}{dx} dx.$$

This means that pressure loss due to acceleration is given by:  $AdF = p_a(x) - p_a(x + dx)$  which leads to

$$\frac{dp_a}{dx} = -2 \frac{\rho}{A^2} Q \frac{dQ}{dx}. \quad (2.9)$$

All the equations which are derived can be combined to only one differential equation. Combining the equations (2.1) and (2.2) and one differentiation gives:

$$\frac{d^2 Q}{dx^2} = J_s \frac{dp_w}{dx},$$

after using equation (2.3) the following equation appears:

$$\frac{d^2 Q}{dx^2} = J_s \left[ \frac{dp_f}{dx} + \frac{dp_a}{dx} \right].$$

Replacing  $\frac{dp_f}{dx}$  and  $\frac{dp_a}{dx}$ , by using the equations (2.4) and (2.9), gives the final differential-equation:

$$\frac{d^2 Q}{dx^2} = \frac{J_s \rho}{A^2} \left[ \left( 1 + \lambda d \frac{1}{Q} \frac{dQ}{dx} \right) \frac{f(Q)}{2d} Q^2 - 2Q \frac{dQ}{dx} \right]. \quad (2.10)$$

As one can see, the model is a second order differential equation. This means that each solution has two degrees of freedom and, therefore, two boundary conditions are required for a unique solution and should be prescribed. It should be noted that two boundary conditions are necessary for a unique solution but it does not have to be sufficient. It is possible to prescribe two boundary conditions in one point, but this would result in a code in which the well length can not be used anymore as an input parameter. This would be a great restriction, therefore, one of the conditions will be prescribed at the heel and the other will be prescribed at the toe. As boundary condition we can use the production rate in a certain point or the derivative of the production rate in that point. It should be noted that according to eq. (2.1), that prescribing the value of the mentioned derivative is the same as prescribing the drawdown. One of the following two next boundary conditions can be prescribed at the heel:

$$Q(0) = Q_0$$

or

$$\frac{dQ}{dx}(0) = Q'_0.$$

If the drawdown at the heel is given by  $\mathcal{D}_0$  then the relation between the drawdown at the heel and the derivative at the heel is given by:

$$Q'_0 = -J_s \mathcal{D}_0.$$

Similarly, for the toe the options for the boundary conditions become:

$$Q(L) = Q_L$$

or

$$\frac{dQ}{dx}(L) = Q'_L$$

leading to

$$Q'_L = -J_s \mathcal{D}_L.$$

## 2.3 Model properties

Before trying to find the numerical solution, it is useful to gain a bit more insight in the model and the solution. Therefore, this section contains a small investigation on the magnitudes of the different types of pressure drop in the well. It is useful to know how large the relative importance of the contributions to pressure loss are. After this comparison, a small research on the solution of the model follows. This investigation on the model solutions provides the reader with more insight into the solution.

If one takes a look at eq. (2.9) and eq. (2.5) one can see that the correction of the frictional pressure drop for the inflow compared to the pressure drop in a pipe without inflow, can be written as

$$25d \frac{1}{Q} \frac{dQ}{dx}.$$

A typical value of  $Q(x)$  is given by  $\tilde{Q}$  and the length scale on which significant changes in  $\tilde{Q}$  occur is denoted as  $\Delta l$ . This means that the derivative of  $Q$  can be written as

$$\frac{dQ}{dx} = O\left(\frac{\tilde{Q}}{\Delta l}\right).$$

Therefore, the influence of the inflow on the frictional pressure drop compared to the total pressure drop in a pipe without the inflow can be written as

$$\frac{25d}{\Delta l}.$$

In order to obtain a significant influence of the inflow on the friction in the pipe, the typical length scale should be of order  $25d$ , that is

$$\Delta l = 25d.$$

Calculations later will show that significant changes in  $\tilde{Q}$  occur on a lengthscale of order  $L$ . If the well length is given by  $L = 1000\text{m}$  and the diameter of the well is  $16\text{cm}$ , then the relative importance of the correction for the inflow compared to the total pressure drop in a pipe without the inflow is given by

$$25d \frac{1}{Q} \frac{dQ}{dx} = 5 \cdot 10^{-3}.$$

Therefore, no significant error will be included if the correction for the inflow is not taken in account. So, it is ignored in the following of this report, unless mentioned otherwise. It is also possible to compare the contribution of the acceleration with the friction. After using the equations (2.9) and (2.5) it follows that the accelerational pressure drop compared to the frictional pressure drop can be written as

$$\frac{dp_a}{dx} / \frac{dp_f}{dx} = \frac{4d}{f(Q)Q} \frac{dQ}{dx}.$$

After some calculations and using the following typical value for the friction factor,  $f(Q) = 2 \cdot 10^{-2}$ , it follows that another way of writing the relative contribution of the acceleration compared to the friction is given by

$$\frac{dp_a}{dx} / \frac{dp_f}{dx} = O\left(\frac{200d}{\Delta l}\right).$$

In order to obtain the same order of magnitude for the friction and acceleration the typical length scale  $\Delta l$  should be of order  $200d$ , that is

$$\Delta l = O(200d).$$

If the well length is given by  $L = 1000\text{m}$  and the diameter of the well is given by  $d = 0.16$ , the relative importance of the accelerational pressure drop compared to the frictional pressure drop can be estimated by

$$\frac{dp_a}{dx} / \frac{dp_f}{dx} = 3 \cdot 10^{-2}.$$

This means that the acceleration is quite small and negligible if necessary. However, this is not done in the calculations, nor in the analysis which are written down in this report.

Furthermore, also the solutions of the model have some interesting properties. These properties can be used for an analysis of the model and are derived with the use of some knowledge of differential equations. First, it will be repeated that two suitable boundary conditions have to be prescribed in order to obtain an unique solution and also that this is necessary but not sufficient. It is possible that there exists no solution for the two prescribed boundary conditions or, that infinitely many solutions for the two given conditions can be found. Assuming that there exists only infinitely many solutions if prescribing one of the conditions automatically forfills the other and that this happens only in extreme cases, it can be said that if a solution is obtained that this one is unique for the two given conditions. The extreme cases are the cases with infinitely long wells and infinitely large or small boundary conditions. Therefore, only finite wells and bounded boundary conditions will be used. This knowledge can be used to derive some interesting and useful properties of the solutions. The first one is an easy one, a finite well with

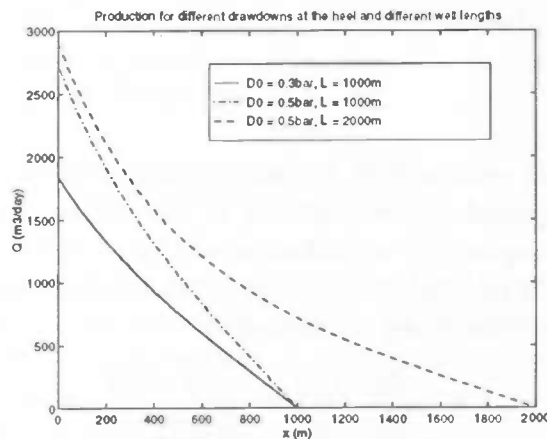


Figure 2.3.1 : Three solutions for different well lengths and different drawdowns at the heel.

$\mathcal{D}_0 > 0$  and  $Q(L) = 0$  has a positive decreasing drawdown and a positive production rate along the well. The drawdown can not become equal to zero at some point  $x \in (0, L)$  because then  $Q = 0$  at  $[0, L]$  has to yield. Therefore, the drawdown is always positive and due to the pressure drop along the well also decreasing. The next solution feature is almost equal, two solutions of an equal finite well with a different drawdown at the heel have only one equal value, that is  $Q(L) = 0$ . Hence, a higher  $\mathcal{D}_0$  gives a higher drawdown and also a higher production rate along the whole well. The last comparison is made between two wells with equal  $\mathcal{D}_0$ , a different, but finite, well length and equal remaining parameters. The two model solutions can have only one equal value and this is the value for  $\mathcal{D}_0$ . Furthermore, both the solutions have their only root at the toe. These two facts combined gives the longest well the highest production rate everywhere along the well. The last two solution properties are shown in Figure 2.1.3. The figure shows three solutions, these solutions are obtained by using one of the next combinations of the

drawdown at the heel and the well length:  $\mathcal{D}_0 = 3.0 \cdot 10^4 \text{Pa}$ ,  $L = 1.0 \text{km}$ ,  $\mathcal{D}_0 = 5.0 \cdot 10^4 \text{Pa}$ ,  $L = 1.0 \text{km}$  and  $\mathcal{D}_0 = 5.0 \cdot 10^4 \text{Pa}$ ,  $L = 2.0 \text{km}$ , all the other remaining parameters solution are equal for the three solutions. It can be seen that if the three solutions are compared pairwise, that they have only one corresponding value:  $Q(L)$  or  $Dq(0)/dx$ .

## Chapter 3

# Numerical solution of the model

### 3.1 Linearisation

The model equations have been derived. Since the final model equation turn out to be a non-linear differential equation, the equations will be linearised. For convenience  $\frac{f(Q)}{2d}$  is replaced by  $\hat{f}(Q)$ . The linearisation is done by the method of Newton, this is a common iteration method for root finding problems. The iteration process for finding a root of a function,  $f : \mathfrak{R} \rightarrow \mathfrak{R}$  is given by

$$x^{(n+1)} = x^{(n)} - \frac{f(x^{(n)})}{f'(x^{(n)})},$$

with  $x^{(n)}$  the approximation of the root after  $n$  iteration steps. The iteration process starts with an initial guess, which hopefully leads to an accurate approximation of a root of the function  $f(x)$ . The Newton-method is a quadratic convergent iteration scheme which means that the error in  $x^{(n+1)}$  is the square of the error in  $x^{(n)}$ . The method can also be applied to give an iterative solution for non linear-differential equations.

The root of the function  $F(Q) : C^2[0, L] \rightarrow \mathfrak{R}$ , with

$$F(Q) = \frac{d^2Q}{dx^2} - \frac{J_s \rho}{A^2} [ \hat{f}(Q)Q^2 - 2Q \frac{dQ}{dx} ], \quad (3.1)$$

is a solution of equation (2.10), with  $\lambda = 0$  subjected to admissible boundary conditions. The iteration process for the funtion  $F(Q)$  can be defined in the following way:

$$F'(Q^{(n)})[Q^{(n+1)}] = F'(Q^{(n)})[Q^{(n)}] - F(Q^{(n)}), \quad (3.2)$$

in which  $F'(Q^{(n)})[Q^{(n+1)}]$  denotes a functional derivative. This derivative is given by:

$$F'(\phi)[\psi] = \lim_{\epsilon \rightarrow 0} \frac{F(\phi + \epsilon\psi) - F(\phi)}{\epsilon}. \quad (3.3)$$

These last two equations can be used to find a second order convergent iteration scheme for  $F(Q)$ . This gives the following iteration formula:

$$Q_{xx}^{(n+1)} + 2\frac{J_s\rho}{A^2}Q^{(n)} \cdot Q_x^{(n+1)} - \frac{J_s\rho}{A^2}Q^{(n)} \left[ 2\hat{f}^{(n)} + Q^{(n)}\frac{d\hat{f}^{(n)}}{dQ} \right] \cdot Q^{(n+1)} =$$

$$2\frac{J_s\rho}{A^2}Q^{(n)}Q_x^{(n)} - \frac{J_s\rho}{A^2}Q^{(n)2} \left[ \hat{f}^{(n)} + Q^{(n)}\frac{d\hat{f}^{(n)}}{dQ} \right], \quad (3.4)$$

with

$$\hat{f}^{(n)} = \hat{f}(Q^{(n)})$$

and

$$\frac{d\hat{f}^{(n)}}{dQ} = \frac{d\hat{f}^{(n)}Q^{(n)}}{dQ}.$$

As one can see, the remaining iteration formula is a linear formula in  $Q^{(n+1)}$ , which can lead to a solution. In order to obtain a unique solution it is necessary that all the iterates  $Q^{(n+1)}$  are subjected to the demanded boundary conditions. It stated that if there is a solution for two bounded boundary conditions and a finite well that the solution is unique. This means that if the iteration process converges, it will converge to the demanded solution and the solution will be unique.

### 3.2 Discretisation

The linearisation of equation (2.10) is the first step which leads to the final solution. The second step is the discretisation which leads to a discreet approximation of the solution of the linearised equation. The discretisation is done on a uniform grid with  $N$  cells. The first calculation point is taken at  $x = 0$  and the last one in  $x = L$ . The nodes in between are given by:  $x_i = i \cdot h$ ,  $i = 0, \dots, N$  with  $h = \frac{L}{N}$  denoted as the mesh width of the grid. The solution of the linearised equation is denoted as  $Q^{(n+1)}$  and its discreet approximation will be denoted as  $Q^{(n+1)}$ , with  $Q_i^{(n+1)}$  as the discreet approximation of  $Q^{(n+1)}(x_i)$ . The derivatives are approximated by using second order central discretisation methods. The formulas for the central second order discretisation methods for  $Q''(x_i)$  and  $Q'(x_i)$  are given by:

$$\frac{d^2Q}{dx^2}(x_i) = \frac{Q_{i+1} - 2Q_i + Q_{i-1}}{h^2} + O(h^2) \quad (3.5)$$

and

$$\frac{dQ}{dx}(x_i) = \frac{Q_{i+1} - Q_{i-1}}{2h} + O(h^2). \quad (3.6)$$

An extended analysis of the discretisation methods can be found in [KA, 1978].

Using these discretisation formulas in equation (3.4) leads to the following equations for all the inner nodes:

$$l_i^{(n)}Q_{i-1}^{(n+1)} + d_i^{(n)}Q_i^{(n)} + u_i^{(n)}Q_{i+1}^{(n+1)} = r_i^{(n)}, \quad \forall i = 1, \dots, N-1, \quad (3.7)$$

with

$$l_i^{(n)} = \frac{1}{h^2} - \frac{J_s \rho}{A^2} \frac{Q_{i-1}^{(n)}}{h}, \quad (3.8)$$

$$d_i^{(n)} = -\frac{2}{h^2} - \frac{J_s \rho}{A^2} Q_i^{(n)} \left[ 2\hat{f}_i^{(n)} + Q_i^{(n)} \frac{\Delta \hat{f}_i^{(n)}}{\Delta Q_i^{(n)}} \right], \quad (3.9)$$

$$u_i^{(n)} = \frac{1}{h^2} + \frac{J_s \rho}{A^2} \frac{Q_{i+1}^{(n)}}{h} \quad (3.10)$$

and

$$r_i^{(n)} = \frac{J_s \rho}{A^2} \left[ \frac{Q_{i+1}^{(n)} - Q_{i-1}^{(n)}}{h} - Q_i^{(n)2} \hat{f}_i^{(n)} - Q_i^{(n)3} \frac{\Delta \hat{f}_i^{(n)}}{\Delta Q_i^{(n)}} \right]. \quad (3.11)$$

The following notation was used in the above equations

$$\hat{f}_i^{(n)} = \hat{f}(Q_i^{(n)})$$

and

$$\frac{\Delta \hat{f}_i^{(n)}}{\Delta Q_i^{(n)}} = \frac{\hat{f}(Q_{i+1}^{(n)}) - \hat{f}(Q_{i-1}^{(n)})}{Q_{i+1}^{(n)} - Q_{i-1}^{(n)}}.$$

The coefficients  $l_i^{(n)}$ ,  $d_i^{(n)}$ ,  $u_i^{(n)}$  and  $r_i^{(n)}$  will change at the edges of the grid. How the boundary coefficients change depends on the type of boundary condition at the corresponding boundary node. The Dirichlet boundary conditions are the easiest to deal with. Just replace  $Q_i^{(n)}$  by its described value, this is  $Q_0$  in  $x = 0$  and  $Q_L$  in  $x = L$ . The following coefficients for a Dirichlet boundary condition in  $x = 0$  show up after calculation:

$$\begin{aligned} l_0^{(n)} &= 0, \\ d_0^{(n)} &= 0, \\ u_0^{(n)} &= 0, \\ r_0^{(n)} &= 0, \\ r_1^{(n)} &= r_1^{(n)} - l_1^{(n)} Q_0 \end{aligned}$$

and

$$l_1^{(n)} = 0.$$

The treatment of a Dirichlet boundary condition in  $x = L$  which prescribes  $Q(L) = Q_L$  is similar:

$$\begin{aligned}
r_{N-1}^{(n)} &= r_{N-1}^{(n)} - u_{N-1}^{(n)} \cdot Q_L, \\
u_{N-1}^{(n)} &= 0, \\
l_N^{(n)} &= 0, \\
d_N^{(n)} &= 0, \\
u_N^{(n)} &= 0
\end{aligned}$$

and

$$r_N^{(n)} = 0.$$

The Neumann boundary conditions which are obtained when the drawdown is prescribed are a bit more complicated. The problem is caused by the discretisation over the edge of the grid. For example, this results in an appearance of  $Q_{-1}^{(n)}$  in the coefficients  $d_0^{(n)}$  and  $r_0^{(n)}$  at  $x = 0$ . Therefore, the value of  $Q_{-1}^{(n)}$  has to be removed. This can be achieved by using the prescribed value of  $Q_x(0)$  and equation (3.6). After the removal of  $Q_{-1}^{(n)}$  the following coefficients are obtained:

$$\begin{aligned}
l_0^{(n)} &= 0, \\
d_0^{(n)} &= -\frac{2}{h^2} + \frac{J_s \rho}{A^2} \left[ 2Q'_0 - 2Q_0^{(n)} \hat{f}_0^{(n)} + Q_0^{(n)2} \frac{\Delta \hat{f}_0^{(n)}}{\Delta Q_0^{(n)}} \right], \\
u_0^{(n)} &= \frac{2}{h^2},
\end{aligned}$$

and

$$r_0^{(n)} = \frac{2Q'_0}{h} - \frac{J_s \rho}{A^2} Q_0^{(n)2} \left[ \hat{f}_0^{(n)} + Q_0^{(n)} \frac{\Delta \hat{f}_0^{(n)}}{\Delta Q_0^{(n)}} \right],$$

$$\text{with } \frac{\Delta \hat{f}_0^{(n)}}{\Delta Q_0^{(n)}} = \frac{\hat{f}(Q_1^{(n)}) - \hat{f}(Q_{-1}^{(n)} - 2hQ'_0)}{2hQ'_0}.$$

The derivation of the coefficients is similar in the case of a Neumann boundary condition at  $x = L$ . This leads to the following coefficients:

$$\begin{aligned}
l_N^{(n)} &= \frac{2}{h^2}, \\
d_N^{(n)} &= -\frac{2}{h^2} + \frac{J_s \rho}{A^2} \left[ 2Q'_L - 2Q_N^{(n)} \hat{f}_N^{(n)} + Q_N^{(n)2} \frac{\Delta \hat{f}_N^{(n)}}{\Delta Q_N^{(n)}} \right], \\
u_N^{(n)} &= 0
\end{aligned}$$

and

$$r_N^{(n)} = -\frac{2Q'_L}{h} - \frac{J_s \rho}{A^2} Q_N^{(n)2} \left[ \hat{f}_N^{(n)} + Q_N^{(n)} \frac{\Delta \hat{f}_N^{(n)}}{\Delta Q_N^{(n)}} \right],$$

$$\text{with } \frac{\Delta \hat{f}_N^{(n)}}{\Delta Q_N^{(n)}} = \frac{\hat{f}(Q_{N-1}^{(n)} + 2hQ'_L) - \hat{f}(Q_{N-1}^{(n)})}{2hQ'_L}$$

After using the formulas for the boundary points, it is possible to put the equations (3.7) into a linear system, which leads to:

$$A^{(n)} Q^{(n)} = r^{(n)}. \quad (3.12)$$

For a Neumann boundary condition at  $x = 0$  and a Dirichlet boundary condition at  $x = L$ , the matrix  $A^{(n)}$  is a tridiagonal matrix with lower diagonal  $[l_1^{(0)}, \dots, l_{N-1}^{(n)}]$ , diagonal  $[d_0^{(0)}, \dots, d_{N-1}^{(n)}]$  and upper diagonal  $[u_0^{(0)}, \dots, u_{N-2}^{(n)}]$ . It is clear that the size of the matrix depends on the type of boundary conditions, but for all possible boundary conditions one obtains a tridiagonal which can be solved by using Gauss elimination. It is required for a unique and physical solution that all the matrix coefficients remain bounded during the iteration process, it is shown in Appendix C that this does not have to be a problem.

# Chapter 4

## Results

### 4.1 Numerical analysis and results

It is claimed in section 2.2 and section 2.3 that the solution method has a quadratic speed of convergence and a second order discretisation error. In order to substantiate this claim, several simulations have been done with common values for the input parameters. The iteration process reaches its desired accuracy after only a few iterations, usually only five steps. In order to have a quadratic iteration scheme, it is required that for the relative difference of two succeeding solutions,

$$\delta Q^{(n)} \equiv \frac{\|Q^{(n+1)} - Q^{(n)}\|}{\|Q^{(n)}\|},$$

should yield :

$$\delta Q^{(n+1)} = \delta Q^{(n)2},$$

which is equivalent with

$$\frac{\log(\delta Q^{(n+1)})}{\log(\delta Q^{(n)})} = 2.$$

Figure 4.1.1 shows a plot of  $\log(\delta Q^{(n+1)})/\log(\delta Q^{(n)})$  versus the number of iterations. As the results show, the value tends to its theoretical value after a few steps. The fact that after a few steps the speed of convergence becomes smaller than its desired value might be caused by rounding errors, but it is clear that the process converges quadratically.

Only second order discretisation methods are used for the discretisation of the linearised version of the model. The discretisation error,  $e_{(h)}$  is defined as the numerical integrand of the difference between the real and calculated solution. This integration is done with the Simpson rule and results in :

$$e_{(h)} = c_1 \cdot h^2, \quad c_1 \in \mathfrak{R}. \quad (4.1)$$

If  $Q_{(h)}$  is the solution which belongs to mesh width  $h$  then one can write,

$$\|Q_{(h)} - Q_{(2h)}\| = \|e_{(h)} - e_{(2h)}\|,$$

it follows that equation (4.1) is equivalent with

$${}^2 \log \frac{\|Q_{(4h)} - Q_{(2h)}\|}{\|Q_{(2h)} - Q_{(h)}\|} = 2.$$

Figure 4.1.2 shows the order of the discretisation error,

$${}^2 \log \frac{\|Q_{(4h)} - Q_{(2h)}\|}{\|Q_{(2h)} - Q_{(h)}\|}$$

versus the mesh width. It is clear that the obtained value for the order is very close to the desired, theoretical value. So one can conclude that the discretised version of the linearised model has a second order discretisation error.

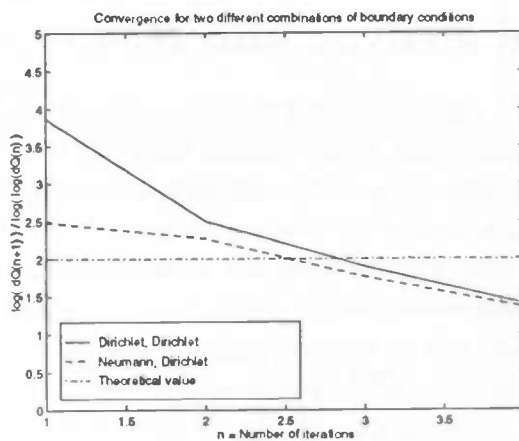


Figure 4.1.1 : The speed of convergence versus the number of iterations, for different combinations of boundary conditions.

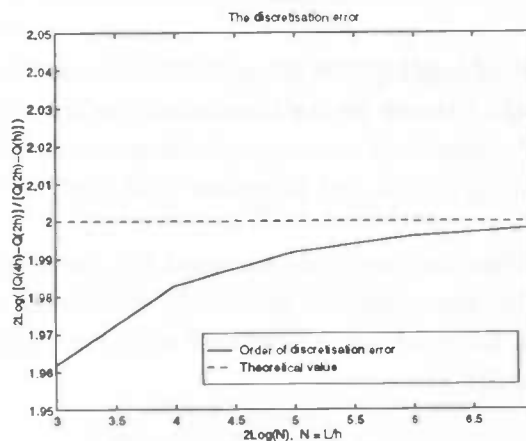


Figure 4.1.2 : The discretisation error as a function of the mesh width.

## 4.2 Model analysis

### 4.2.1 Introduction

In order to gain more insight into the production characteristics of horizontal wells, an extended analysis of the sensitivity and influence of some parameters is necessary. This is done by running simulations and changing only one parameter at the time, while the other parameters keep their same (standard) value. The standard values for the parameters are shown in Table 4.2.1.1.

$\rho$	=	fluid density	:	781.0kg/m <sup>3</sup>
$\mu$	=	fluid viscosity	:	1.32cP
$d$	=	pipe diameter	:	0.16m
$J_s$	=	specific productivity index	:	10.0Sm <sup>3</sup> /day/bar/m
$L$	=	well length	:	1000.0m
$f(Q)$	=	type of friction factor	:	Haaland
$\epsilon$	=	roughness parameter	:	0.0m
$h$	=	cell length	:	25m
$\mathcal{D}_0$	=	drawdown at the heel	:	0.3bar
$Q_L$	=	production rate at the toe	:	0.0m <sup>3</sup> /s

**Table 4.2.1.1** : List with the standard values for the parameters.

The cell length,  $h = 25\text{m} \sim N = 40$  points, is chosen in such a way that the difference in the solution is less than 1% compared to the solution for a small  $h$ , like  $h = 0.5\text{m}$ . While SI-units are used in the developed code, for input and output purposes we allow other units. The unit for the production rate on the plots for example is chosen as m<sup>3</sup>/day and not as m<sup>3</sup>/s. This choice is made because the presented units are more common in the oil world.

The parameter study is divided into two groups. The first group contains only the analysis of influence of the drawdown on several output quantities. The other group contains an analysis of all the other parameters which appear in the model.

### 4.2.2 Analysis of the drawdown

Some production profiles for different drawdowns at the heel are shown in Figure 4.2.2.1. This plot can be used to describe some physical aspects about the well flow and to analyse the influence of the drawdown at the heel.

If the drawdown at the heel is positive then the first aspect that can be seen is the increase of the production rate towards the heel. It is shown in section 2.3 that a positive drawdown at the heel gives a positive drawdown along the whole well and, therefore, inflow along the whole well. Since the toe is closed, the oil has to move towards the heel.

It can also be seen in Figure 4.2.2.1, that the production profile curve become more

steep towards the heel, i.e. the inflow increases slightly towards the heel. This is caused by the pressure drop due to the friction and acceleration effects. As a result of this pressure drop, the drawdown reduces if one moves from the heel towards the toe. Via the equations (2.1) and (2.2) it follows that the friction and the acceleration give a small increase of the inflow towards the heel.

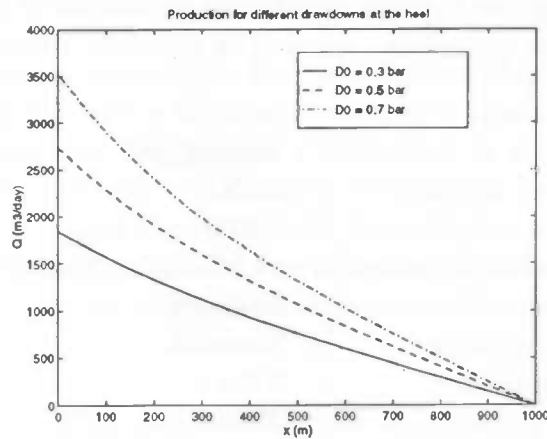


Figure 4.2.2.1 : Production profiles for different drawdowns at the heel.

Simulations show that an increase of the drawdown at the heel does not lead to the same relative increase in the total production rate, i.e. the relative increase in the total production rate is smaller than the relative increase in the drawdown at the heel. This can be seen in Figure 4.2.2.2, this figure shows a plot of the total production rate as a function of the drawdown at the heel. As one can see, the slope of this  $D_0$ - $Q_0$ -curve decreases if the drawdown at the heel increases. In the preceding ainea it was mentioned that a higher drawdown at the heel gives a higher drawdown and production rate along the whole well. This means that the pressure drop increases, especially at the heel. Therefore, the increase in the drawdown along the well is smaller than the increase in the drawdown at the heel. This results in a relative smaller increase in the total production rate than in the drawdown at the heel.

It is possible to make a good least squares fit for the  $D - Q(0)$  relation for the used parameters. This third degree polynomial fits very good if the drawdown at the heel is between 0.0bar and 0.9bar and is given by:

$$Q_0 = D \cdot [ c_1 D^2 + c_2 D + c_3 ],$$

with  $c_1 = 4.2 \cdot 10^3$ ,  $c_2 = -7.5 \cdot 10^3$  and  $c_3 = 8.1 \cdot 10^3$ .

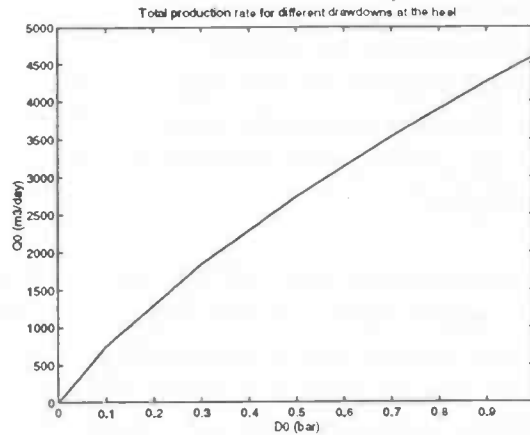


Figure 4.2.2.2 : Total production rate as a function of the drawdown at the heel.

The next plot shows the total pressure loss per meter caused by friction and acceleration. As one can see, the biggest drop appears at the heel and decreases slowly if one moves towards the toe. The figure shows that the total pressure loss along the well has the same magnitude as the drawdown at the heel, which was  $\mathcal{D}_0 = 0.3\text{bar}$ . This means that the pressure loss in the well can not be ignored if the input values of Table 4.2.1.1 are used. It is shown in section 2.3 that the pressure loss caused by friction is much larger than the pressure loss caused by acceleration, this can also be seen in Figure 4.2.2.3.

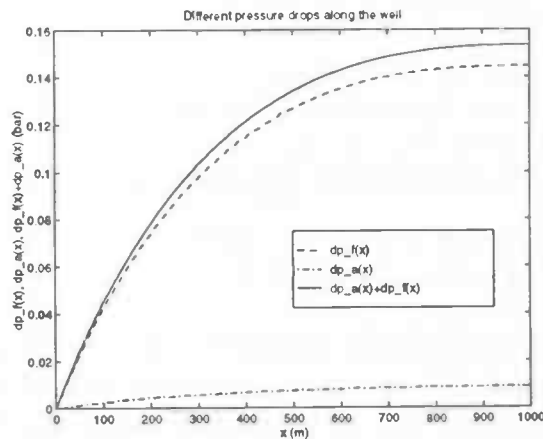


Figure 4.2.2.3 : Different pressures along the well with  $\mathcal{D}_0 = 0.3\text{ bar}$ .

### 4.2.3 Analysis of the other parameters

The drawdown at the heel is the only parameter that can be controlled during the production process. The parameters like the well length and the diameter of the production pipe can not be changed during the production process. This means that all the information available should be combined together with the knowledge obtained from the models of the well length and the pipe diameter in order to choose them as best as possible. The other parameters that are investigated in this section are the specific productivity index,

the roughness and the viscosity. They can not be chosen and the specific productivity index and roughness are also quite hard to measure. This means that it is quite important to know how sensitive the total production rate and the inflow distribution is to changes in one of these parameters. The last appearing parameter in the model is the density of the fluid. The influence of the fluid density will not be large for the possible densities between  $700\text{kg/m}^3$  and  $1000\text{kg/m}^3$

A longer well gives more production, but will also have higher production costs, so it is interesting to see how the inflow behaves if the well is made longer. Three production profiles for three different well lengths and a drawdown at the heel of  $\mathcal{D}_0 = 0.3\text{bar}$ , are shown in Figure 4.2.3.1. One can see that if a comparison between wells with different lengths is made, that the longer horizontal well has a higher production rate everywhere along the well. But a higher production rate will give also a higher pressure drop, which means that an extension of the well gives a relative smaller increase in total production rate.

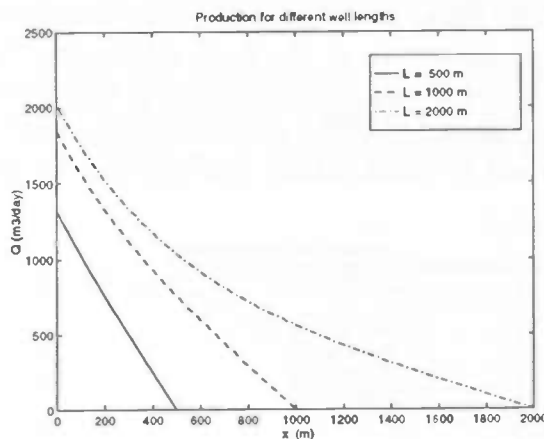
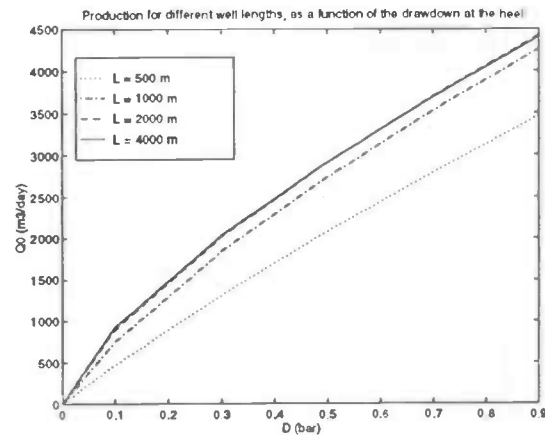


Figure 4.2.3.1 : Production profiles for different well lengths with a constant drawdown at the heel of  $0.3\text{bar}$ .

If one varies the well length and the drawdown, while keeping the values of the other parameters as in Table 4.2.1.1, then one can find that 80% of the production of a well with a length of four kilometers can be reached by using a well with a length of only one kilometer, independent of the drawdown that is used! This effect can also be seen in Figure 4.2.3.2. This figure shows four curves of the total production rate as a function of the drawdown for four different well lengths. It can be seen that the total production rates for different drawdowns at the heel and for  $L = 2000\text{m}$  and  $L = 4000\text{m}$  are almost equal for every drawdown. However, the total production rate for  $L = 1000\text{m}$  is almost the double of the value of the total production rate for  $L = 500\text{m}$ , for every shown drawdown at the heel. The required well length in order to reach 80% of the total production rate of a "very long" well, in this case  $L = 4\text{km}$ , can be seen as the economic length of a well. Is it worth to try to produce the last 20% considering the extra costs. The length of the "very long" well depends on the value of all the parameters, but can easily be found with the developed code.



Different radii of the production pipe give different production profiles. Three of the profiles are demonstrated in Figure 4.2.3.3. It is not clear which diameter gives the most optimal result, so a small analysis on the influence of the diameter of the production pipe is useful. According to the equations eq. (2.9) and eq.(2.4), a larger pipe diameter will give a lower pressure drop. Therefore, a larger pipe radius will increase the total production and give a more even inflow. A common value for the pipe diameter is 0.15m, the production profile for a pipe with this diameter is shown in the plot. Simulations show that for the used well length and used drawdown at the heel, the influence of the pipe diameter is very strong around  $d = 0.16\text{m}$ , a change of the pipe diameter in that area will lead to a relative larger change of the total production rate. In addition, the influence of the pipe radius on the total production rate is very small if the radius is larger than approximately 0.25m for the used well length and drawdown at the heel.

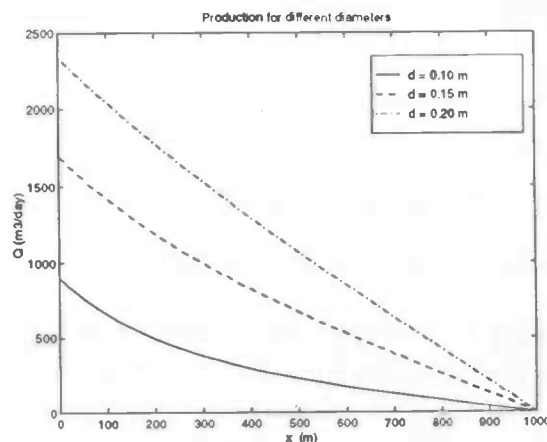


Figure 4.2.3.3 : Production profiles for different diameters of the production pipe.

The production profiles for three different values of the specific productivity index,  $J_s$ , are shown in the Figure 4.2.3.4. It can be seen that a higher  $J_s$  gives a higher production

rate along the well which in addition gives a higher pressure drop. The higher pressure drop reduces the effect of the higher  $J_s$  somewhat and gives also a less even inflow along the well.

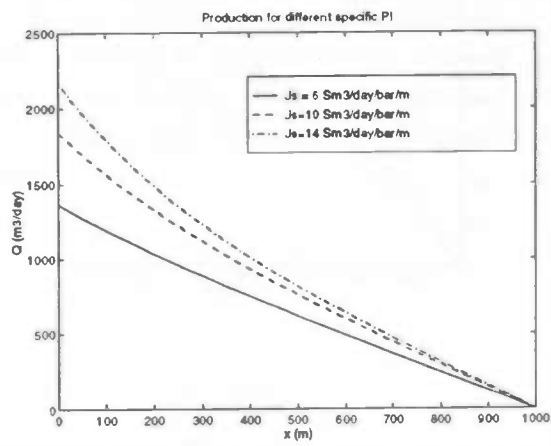


Figure 4.2.3.4 : Production profiles for different productivity indices.

A few production profiles for different roughness of the pipe are shown in Figure 4.2.3.5. The figure shows that a well with a higher roughness  $\epsilon$ , gives a lower total production rate and a less even inflow. Therefore, it should be tried to keep the pipe as smooth as possible.

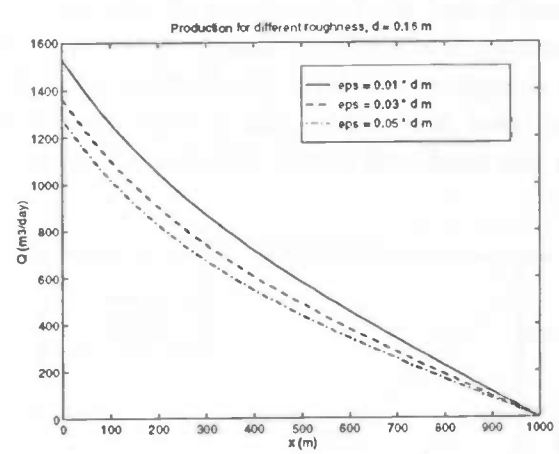


Figure 4.2.3.5 : Production profiles for different values of the roughness parameter.

Some production profiles for different oil viscosities of the oil are shown in Figure 4.2.3.6. The variation in viscosity can be a few orders of magnitude. For example, the production of water can give small drops in the oil which can lead to a large increase of the viscosity. Therefore, it is useful to know how the production reacts to changes in the viscosity. A more viscous fluid will increase the friction quite rapidly and, therefore, gives a smaller total production rate and a less even inflow.

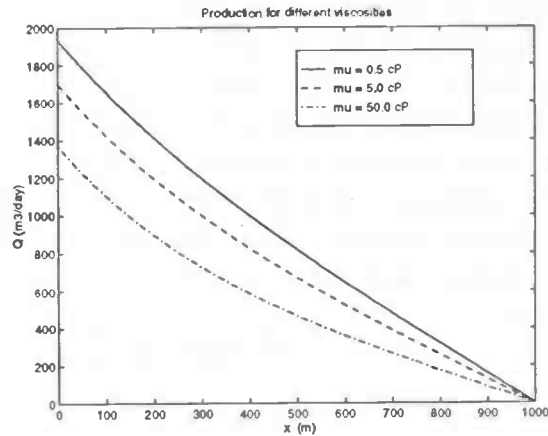


Figure 4.2.3.6 : Production profiles for different viscosities.

### 4.3 A comparison with other models.

The model described in this paper is compared with a model which does not include any pressure drop in the well. The goal of this comparison is to find out for which well length the pressure drop in the well can not be ignored. The standard values for the other parameters of Table 4.2.1.1 are used for this comparison. The total production rate in the "no pressure drop" approach, is calculated by the following formula :

$$Q_0 = PI \cdot D,$$

with

$$PI = J_s \cdot L.$$

The formula for the  $PI$  is not the same one as the one used in [SJ,1987], [SJ,1988] or [GR,1984]. The formula given by these people could not be applied because there was not enough information available on the determination of the productivity index.

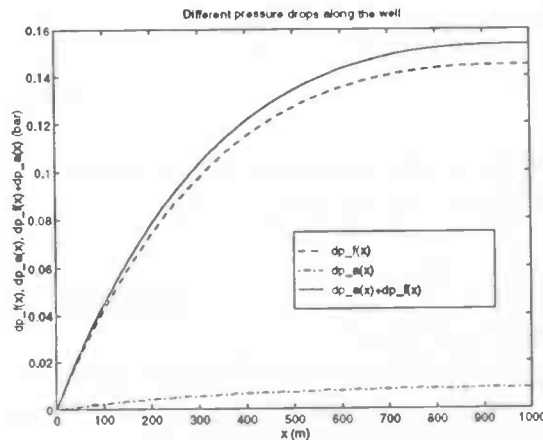


Figure 4.3.1 : The total production rate for different well lengths, for different approaches.

The total production rate for different well lengths for the two compared models is given in Figure 4.3.1. The figure shows that the difference between the two different models becomes significant if  $L > 500\text{m}$ . This well length depends on all the used parameters but shows that after a certain length, which will be significantly smaller than the well length, the pressure drop in the well has a significant influence on the total production rate. In the preceding two sections it was described what the influence of the different parameters was on the production profile. All the changes that result in a higher pressure drop, i.e. give a less even inflow, will decrease the maximum value of  $L$  for which the pressure drop can be ignored.

# Chapter 5

## An extended model

### 5.1 Introduction

In the model that was developed in section 2.1, it was assumed that the inflow depends linear on the drawdown. The justification for this assumption is given in Appendix A by using Darcy's equation, but is only valid when the pressure drop through the wall of the pipe is negligible compared to the drawdown. This means that the linear equation for the inflow (eq. (2.2)) is not valid any more when the pressure through the pipe wall becomes significant. The pressure drop through the pipe wall becomes important if the flow through the perforations occurs with a high speed, i.e when the relative perforated area of the pipe is small. The relative perforated area of the production pipe is given by the open area of the pipe divided by the total area of the pipe. The calculation of the pressure drop caused by the pipe wall is very difficult, therefore, some experiments with a production pipe with a small relative perforated area were done in order to investigate the pressure loss through the pipe wall. The experiments were done at Norsk Hydro in 1996 by Rinde *et al* and are described in [RU, 1996]. The results show that the pressure loss through the pipe is only important when the relative perforated area is small,  $\sim 10^{-4}$ . The flow through the perforations does not depend linear on the pressure difference between the well and the reservoir if the pressure drop due to the pipe wall is important. Therefore, for the extended version of the model, assumption 6 that was given in section 2.1 will be replaced by the following one:

- 6' : The inflow is determined by the combined effects of the pressure drop in the reservoir and the pressure drop caused by the wall of the pipe.

### 5.2 Model equations

Assuming that the flow through the pipe wall can cause a significant pressure drop, the pressure difference between the well and the reservoir can be written in terms of the flow resistance in the reservoir and the induced pressure loss resulting from the flow through the perforations. Therefore, the pressure drop between the well and the reservoir is written

as

$$p_d - p_w(x) = \Delta p_{res}(x) + \Delta p_{pipe}(x). \quad (5.1)$$

The flow in the reservoir experiences resistance on its way to the pipe. The pressure difference needed in order to get the fluid in the pipe is given by:

$$\Delta p_{res}(x) = \frac{q(x)}{J_s}, \quad (5.2)$$

with

$\Delta p_{res}(x)$  = the part of the drawdown which is used for the movement of the flow in the reservoir.

The part of the pressure loss due to the flow through the perforations depends on the absolute value of the fluid velocity in the perforations. Therefore, the pressure drop caused by the flow through the perforations is given by

$$\Delta p_{pipe}(x) = \frac{1}{2} \rho c_f [v_{per}(x)]^\gamma, \quad (5.3)$$

with

$\Delta p_{pipe}(x)$  = the part of the total pressure loss due to the flow through the pipe wall.  
 $v_{per}(x)$  = the velocity of the flow in the perforations.  
 $c_f$  = the friction coefficient.  $[(m/s)^{2-\gamma}]$   
 $\gamma$  = pipe wall constant, usually in the range  $\gamma \in [1, 2]$

The fluid velocity in the perforations depends on the relative perforated area of the pipe and the volume flux into the pipe. The relative perforated area,  $R_{pa}$ , is given by :

$$R_{pa} = \frac{N_{per} \cdot A_{per}}{\pi d},$$

with

$N_{per}$  = the number of perforations per unit length.  
 $A_{per}$  = the area of one perforation.

The relative perforated area makes it possible to calculate the fluid velocity in the perforations. Given a radial volume flux  $q(x)$ , it follows via a mass balance that

$$v(x)_{per} = \frac{q(x)}{\pi d R_{pa}}. \quad (5.4)$$

Using the the equations (5.1), (5.2) and (5.4) gives the following equations for the inflow-pressure difference equation.

$$p_d - p_w(x) = \frac{q(x)}{J_s} + \sigma q^\gamma(x), \quad (5.5)$$

with

$$\sigma = \frac{\frac{1}{2}\rho c_f}{(\pi d R_{pa})^\gamma}$$

Before calculating the final model equation it should be noted that the  $R_{pa}$  does not have to be constant, i.e. the relative perforated area might be a function of  $x$ . Equations eq.(2.4) and eq.(2.9) that describe the pressure drop in the pipe remain the same. Also the relation between the production rate and the inflow rate, see eq. (2.2), does not change. Using the same steps and notation for the friction as the one described in the last part of section 2.2 gives the following equation, which describes the model with non-linear inflow.

$$\frac{d^2 Q}{dx^2} + \gamma J_s \sigma \left[ -\frac{dQ}{dx} \right]^{\gamma-1} \left[ \frac{d^2 Q}{dx^2} - \frac{R'_{pa}}{R_{pa}} \frac{dQ}{dx} \right] = \frac{J_s \rho}{A^2} \left[ \hat{f}(Q) Q^2 - 2Q \frac{dQ}{dx} \right]. \quad (5.6)$$

As one can conclude from (5.5), the inflow-drawdown equation remains linear if  $\gamma = 1$ . But in order to get back to the original model of section 2, requires also a constant  $R_{pa}$ . In that case, the pressure drop through the perforations can be taken into account by using a smaller specific PI.

### 5.3 Numerical solution of the model

In order to be able to solve for eq. (5.6), the model equation has to be linearised. The linearisation method that is used in section 3.1 is applied to the differential equation and one can find after some calculations that the linearised equation looks like :

$$C_1^{(n)} Q_{xx}^{(n+1)} + C_2^{(n)} Q_x^{(n+1)} + C_3^{(n)} Q^{(n+1)} = R^{(n)}, \quad (5.7)$$

with

$$C_1^{(n)} = \left[ 1 + \gamma J_s \sigma \left[ -Q_x^{(n)} \right]^{\gamma-1} \right],$$

$$C_2^{(n)} = \left[ 2 \frac{J_s \rho}{A^2} Q^{(n)} + \gamma J_s \left[ -Q_x^{(n)} \right] \left[ (1 - \gamma) Q_{xx}^{(n)} + \gamma Q_x^{(n)} \frac{R'_{pa}}{R_{pa}} \right] \right],$$

$$C_3^{(n)} = -\frac{J_s \rho}{A^2} Q^{(n)} \left[ 2 \hat{f}^{(n)} + Q^{(n)} \frac{d\hat{f}^{(n)}}{dQ} \right]$$

and

$$R^{(n)} = -\frac{J_s \rho}{A^2} Q^{(n)} \left[ Q^{(n)} \hat{f}^{(n)} + Q^{(n)2} \frac{d\hat{f}^{(n)}}{dQ} - 2Q_x^{(n)} \right] +$$

$$(1 - \gamma) \gamma J_s \sigma \left[ -Q_x^{(n)} \right]^{\gamma-1} \left[ \frac{R'_{pa}}{R_{pa}} Q_x^{(n)} - Q_{xx}^{(n)} \right].$$

Equation (5.7) is a linear differential equation which can be solved by using the finite difference method. The used second order central discretisations are described in section 3.1 and [KA, 1978]. After the discretisation with use of (3.6) and (3.5) one obtains again a linear system like equation (3.12). This system can then be solved by means of Gauss elimination. The matrix coefficients of the matrix  $A^{(n)}$ ,  $l_i^{(n)}$ ,  $d_i^{(n)}$  and  $u_i^{(n)}$ , and the right hand side  $r_i^{(n)}$ , can be determined via the discretisation of eq. (5.7). Not all the possibilities for the matrix coefficients will be written down, only the coefficients for the inner nodes will be shown. The discretisation becomes rather easy if one use the formulas for  $A^{(n)}$ ,  $B^{(n)}$ ,  $C^{(n)}$  and  $R^{(n)}$ , the coefficients for the inner nodes become :

$$l_i^{(n)} = C_{1,i}^{(n)} \frac{1}{h^2} - C_{2,i}^{(n)} \frac{1}{2h},$$

$$d_i^{(n)} = -2C_{1,i}^{(n)} \frac{1}{h^2} + C_{3,i}^{(n)},$$

$$u_i^{(n)} = C_{1,i}^{(n)} \frac{1}{h^2} + C_{2,i}^{(n)} \frac{1}{2h}$$

and

$$r_i^{(n)} = R_i^{(n)},$$

with  $C_1^{(n)} = C_1(Q_i^{(n)}, Q_{x,i}^{(n)}, Q_{xx,i}^{(n)})$ , etc.

This equations will change in case of a boundary point, the treatment for the different boundary conditions at the edges of the grid was described in section 3.2. The additional friction term in this extended model makes the model and solution somewhat more complicated, but also more stable because of the more spreaded inflow in the well, i.e. the convection term becomes less important. Therefore, the conditions for a stable solution, which are given in Appendix C for the first model can be used for the extended model.

## 5.4 Model properties

It was written in section 5.1 that the pressure drop caused by the pipe wall, becomes significantly large if the relative perforated area of the pipe is very small. But how small does it have to be? Investigation on the relative importance of the pressure drop due to the pipe wall is therefore next.

It was shown in section 5.2 that the pressure difference between the well and the reseroir can be divided into two parts, one for the friction caused by the pipe wall and one for the resistance that flow experiences in the reservoir. The ratio of these two parts is given by :

$$\frac{\Delta p_{pipe}}{\Delta p_{res}} = J_s \frac{\frac{1}{2} \rho c_f q^{\gamma-1}}{(\pi d R_{pa})^\gamma}$$

In order to get an estimation for this ratio, some typical values are used :  $\gamma = 1.44, c_f = 30.5 \text{ (m/s)}^{2-\gamma}, \rho = 781 \text{ kg/m}^3, J_s = 1.15 \text{ m}^3/\text{s/Pa/m}$  ( $= 10 \text{ m}^3/\text{day/bar/m}$ ) and  $d = 0.16 \text{ m}$ . A typical value for  $q(x) = -Q'(x)$  depends on the typical value for the total production rate,  $\tilde{Q}$ , and the length scale on which the significant changes in  $Q_0$  occur,  $\Delta l$ . These values are given by  $\tilde{Q} = 2 \cdot 10^{-2} \text{ m}^3/\text{s}$  and  $\Delta l = 1 \text{ km}$ , therefore  $q(x) = O(2 \cdot 10^{-5} \text{ m}^3/\text{s/m})$ . From this it follows that the pressure drop in due to the pipe wall has the same order of magnitude as the pressure drop in the reservoir, if

$$R_{pa} = O(10^{-5}).$$

Normally production pipes have a  $R_{pa}$  which is much larger than the calculated value. A more common value for the relative perforated area is given by  $R_{pa} = 0.05$ . If this value is used together with the preceding common values, then the relative contribution of the pressure drop through the pipe compared to the pressure drop in the reservoir is given by :

$$\frac{\Delta p_{pipe}}{\Delta p_{res}} = 2 \cdot 10^{-4}$$

The preceding calculations show that the influence of the pressure drop through the pipe is only important in those cases where the relative perforated area is small enough. The case with interesting applications, use of ICDs, is given and analysed in the next section.

## Chapter 6

# Analysis of the extended model

### 6.1 Introduction

It was shown in section 5.4 that the friction experienced by the inflow is only significant if the relative perforated area of the production pipe is very small. This can be achieved by installing Inflow Control Devices (ICD's) in the production pipe. An ICD can be seen as a flow restriction, the inflow has to go through a few small channels before it reaches the main flow. The small relative perforated area of the ICD's results in a high fluid velocity through the ICD. This high velocity results in a significant pressure loss, which increases if the volume flow increases. The pressure drop can be used in combination with a variable ICD density in order to regulate the inflow from the reservoir into the well. A description of ICDs and the test that have been done with them can be found in [RU,1990].

Inflow Control Devices are used in combination with a double rimmed pipe. The flow from the reservoir enters the annulus between the two pipes via the outer perforated outer pipe, then moves downstream in the direction of the ICD and reaches the main flow, see Figure 6.1.1. The flow into the annulus is determined by the pressure difference between the reservoir and the annulus. The pressure in the annulus is determined by the combination of pressure at the ICD and the pressure loss in the annular section. If the distance between two succeeding ICDs is small compared to the well length, then pressure loss in the annulus is small compared to the pressure difference between the well and the reservoir. If one looks at a well with no ICDs installed, then one can find that the pressure loss over a small section is small compared to the drawdown. Therefore, the use of ICDs can be simulated by the developed model when the pressure drop due to the ICD is taken in account as described in section 5.1. The performed simulations are explained in the next chapter and result in guidelines for the use of ICDs.

The friction that is experienced by the flow depends on three parameters :  $c_f$ ,  $\gamma$  and  $R_{pa}$ . The first two parameters have to be determined by experiments, this results in :

$$\gamma = 1.44$$

and

$$c_f = 30.5$$

The relative perforated area at a position with an ICD can be measured by the total area of the flow channels of the ICD in combination with the distance until the next ICD downstream. This results in a step function which cannot be used in the developed code and therefore the  $R_{pa}$  is made continuous. The other parameters that occur in the developed model get the values that are shown in Table 4.2.1 unless mentioned otherwise.

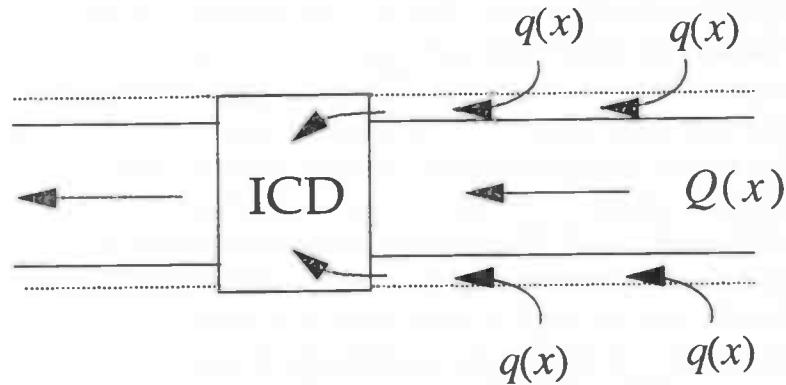


Figure 6.1.1 : The flow in a liner with an ICD installed.

## 6.2 Analysis of the influence of ICD's

In this section an analysis is given of the influence of ICDs on the total production rate and the inflow. This is achieved by simulating a few different ICD distributions along the well. These distributions are converted into a  $R_{pa}$ -function which is used in the model. This function is given by the following parabolic function :

$$R_{pa}(x) = (R_{pa,heel} - R_{pa,toe}) \left( \frac{L-x}{L} \right)^2 + R_{pa,toe}. \quad (6.1)$$

This choice is made because the inflow tends to increase towards the heel, so the flow has to be controlled somewhat stronger over there. The values that are used for the four different test cases are shown below. The value given below in Table 6.2.1 are used in combination with all the other input parameters which are given in Table 4.2.2.1.

case I	: $\mathcal{D}_0 = 0.3\text{bar}$	No use of ICDs		
case II	: $\mathcal{D}_0 = 0.3\text{bar}$	$R_{pa,toe} = 4.6 \cdot 10^{-5}$	$R_{pa,heel} = 4.6 \cdot 10^{-5}$	
case III	: $\mathcal{D}_0 = 0.3\text{bar}$	$R_{pa,toe} = 2.3 \cdot 10^{-5}$	$R_{pa,heel} = 4.6 \cdot 10^{-5}$	
case IV	: $\mathcal{D}_0 = 0.45\text{bar}$	$R_{pa,toe} = 2.3 \cdot 10^{-5}$	$R_{pa,heel} = 4.6 \cdot 10^{-5}$	
case V	: $\mathcal{D}_0 = 0.3\text{bar}$	$R_{pa,toe} = 4.6 \cdot 10^{-6}$	$R_{pa,heel} = 4.6 \cdot 10^{-5}$	

Table 6.2.1 : The values for the five different test cases.

The production profiles of the cases II, III and V are shown in Figure 6.2.1. It can be seen that the use of ICDs results in a lower total production rate, in particular in case

V. Therefore, one must always remember that ICDs can help to regulate the inflow but they result also in a lower total production rate, this is the price that has to be paid for its use. The different inflow patterns for the cases I, III and IV are shown in Figure 6.2.2. If the inflow pattern of *case II* is compared with the one of *case I* then it can be seen that the uniform ICD distribution from *case II* results in a more even inflow along the well. This is due to the pressure loss through the ICD's, which increases when the inflow is high, like in the heel of the well. The  $R_{pa}$ -distribution of *case III* results in an almost equal inflow along the whole well and can therefore be seen as an optimal distribution for the given set of input parameters. The developed code predicts that the drawdown should be increased with about 50% in order to regain the loss of production compared to *case I*. This higher drawdown gives a higher pressure drop and would normally result in a less even inflow pattern, but as one can see in Figure 6.2.2, the differences in inflow along the well are still small. The extra pressure drop induced by the extra production is small compared to the pressure drop through the ICD's and, therefore, has no significant influence. *Case IV* can be used to show that it is quite easy to obtain a  $R_{pa}$  which is too small. The inflow is decreasing towards the heel in this test case, due to the high pressure drop in the ICDs at the heel.

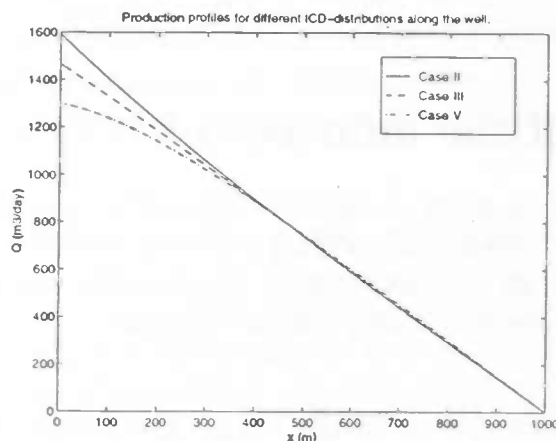


Figure 6.2.1 : The production for the cases II, III and V.

As can be seen in Figure 6.2.2 it is possible to obtain an even inflow for the used set of parameters, but a few guidelines for the choice of the  $R_{pa}$  is more useful. Since all the production profiles without ICDs installed are convex, it might be wise to choose the distribution for the  $R_{pa}$  the same as the one described by eq. (6.1). The optimal distribution is defined as the distribution that results in an even inflow and the lowest possible drawdown as possible, for a given total production rate. In order to get the smallest drawdown, given a fixed total production rate and an even inflow, the value of  $R_{pa,toe}$  should be chosen as large as possible. Now only remains to be found the value of  $R_{pa,heel}$ , this is done with use of the eq. (5.1). The values of  $\mathcal{D}$  and  $q(x)$  at both the heel and the toe can be used in combination with  $R_{pa,toe}$  and  $q(x) = Q_0/L$ . If the total pressure loss in the pipe,  $\mathcal{D}_0 - \mathcal{D}_L$  is known, then the value of  $R_{pa,heel}$  can be calculated

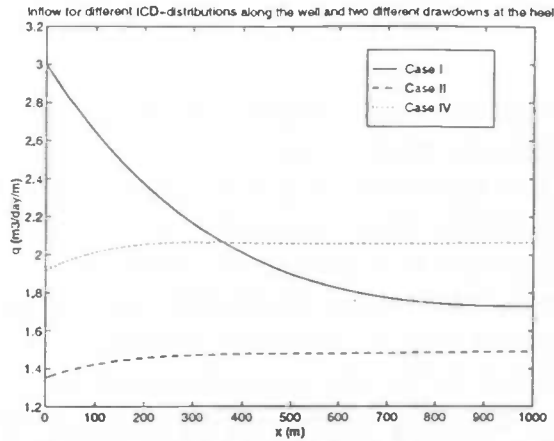


Figure 6.2.2 : The inflow patterns along the well, for the cases I, III and V.

via

$$\mathcal{D}_0 - \mathcal{D}_L = \frac{\frac{1}{2}\rho c_f \frac{Q_0}{L}}{\pi d R_{pa,heel}} - \frac{\frac{1}{2}\rho c_f \frac{Q_0}{L}}{\pi d R_{pa,toe}}$$

Unfortunately, the total pressure loss is not known, however, it can be estimated by the pressure drop in the same well, except that  $R_{pa} \equiv R_{pa,toe}$ . This can be done since the total pressure loss will not change so much if the total production rate remains constant. The function for  $R_{pa}$  than can be converted into an ICD-distribution along the well. It follows via the performed simulations that the 'even inflow situation' is not so sensitive for changes in the drawdown; the calculated  $R_{pa}$  can also be used for other drawdowns.

## Chapter 7

# Discussions, extensions and conclusions

### 7.1 Discussion about the assumptions

Some of the assumptions that were made by Dikken for his model were also used for the derivation of the models that are described in this report. The assumptions made it possible to derive the governing equations, but introduce also limitations of the two models, which were described in this report. Therefore, a discussion about the assumptions listed in section 2.3 is given.

The first assumption, which says that a well contains no differences in height, makes it hard to compare simulations with the measurements obtained from a well, which will often include differences in height. But since this research is done to gain more insight in horizontal wells, this assumption can only be seen as limitation that can be corrected easily if necessary. The next assumption says that the flow inside the well is assumed to be single phase and turbulent. This assumption is an important one, since the flow regime and the type of fluid have a major impact on the pressure drop in the well. However, laminar flow and the transition of laminar to turbulent flow are not included in the model. But it can easily be shown that this simplification will not influence the results significantly. The transition from laminar to turbulent flow happens at a Reynolds number of approximately  $Re = 2000$ . If the values of Table 4.2.1 are used, then the transition happens at  $v = 5 \cdot 10^{-3} \text{m/s} (= 8 \text{m}^3/\text{day})$ . These low values occur only within a small area around the toe. According to the developed code of chapter 2, a drawdown at the heel of 0.3bar and a well length of 1km results in a 5m long laminar section and  $\mathcal{D}_0 = 0.1\text{bar}$  results in a 10m long laminar section. Further simulations show that the laminar section can not be ignored if the total production rate of the well is lower than  $50 \text{m}^3/\text{day}$ , but wells with such a low total productivity rate are generally not interesting. Although the inflow influences the flow structure in the well, its actual influence is small, see section 2.1. The assumption about the single phase can be seen as a crude approximation of the multiphase flow in the well, provided that the different phases in the horizontal section are mixed together and result in a homogeneous fluid with average properties. It should

be noted that a single phase assumption implies also a incompressible fluid. It is assumed that a steady state exists, which is then simulated by the model. There is not so much known about the different time scales during the life of the well, although several different phases seem to exist. The pressure differences in the well in the radial direction are not of major interest and are therefore not included in the model. Although the results would be different if the pressure differences are included, the additional complications are worse than the obtained greater accuracy. It was written in chapter 5.1 that the assumption about the linear relation between the inflow and the drawdown is only valid when then pressure drop through the pipe wall can be ignored. In that case the linear inflow-drawdown relation can be justified by Darcy's equation, see Appendix A. The assumption about the linear flow in the reservoir is only valid for one point, whereas the linear equation (2.9) well. Therefore, it is necessary to assume that the reservoir has constant properties along the well, although it is quite doubtful. But the previous discussed assumption is not enough to get the linear inflow-drawdown equation. One way for obtaining this formula is to assume a constant pressure at a constant distance from the well. This will not be valid in general, especially not when the pressure loss along the well becomes significant. But this assumption combined with the last listed equations results in a constant specific productivity index along the well.

## 7.2 Model extensions

The present model can be extended in several directions. Some of the extensions do not have to be so difficult, while others can make the model very complicated. The first recomodations about model extensions can be achieved by a 1D-model, while the other extensions probably only can be included in a 3D-model.

In general, a well will contain differences in height. The height differences have an influence on the pressure distribution and the inflow along the well. Due to the height differences, the inflow may increase at a certain point. In order to be able to regulate the inflow along a well which contains known height differences, the influence of the hydrostatic pressure can be be investigated. This is just a small extension of the developed models. The biggest limitation of the developed model is the contraction of the whole reservoir into one quantity. A good improvement of the model would be the inclusion of the reservoir flow, especially around the tips of the well. In the best case, this extension leads to a non-constant specific PI, which can easily be included in the developed model. In the worst case, the whole reservoir has to be included in a difficult 3D-way. There can be some places appearing along the well where the diameter of the drilled hole is larger than the diameter of the production pipe, which will lead to an annular flow along the well. As can be seen from measurements, the annular flow gives a concentration of the inflow into the pipe at the heel. The annulus makes it difficult to measure the flow in the reservoir. Although the 1D-model will be somewhat complex, an investigation could be done in order to gain insight. After the start of the production process, the well will become filled with oil. This is the so-called transient behaviour of the well. It might

happen that during the transient behaviour of the well a lot of oil is produced at the heel of the well, therefore, the transient phase of the well might have an influence on the coning process or on other physical aspects. There is relatively little knowledge about transient behaviour for "pressure drop included models", therefore, some energy could be spent in order to obtain the required knowledge. The developed model will be time dependent, but can probably be kept in a 1D-model. The preceding extensions can (perhaps) all be done with a 1D-model, but a lot of extensions can only be done with a 3D-model. Since a lot of possible extensions can be made by a 3D-study, one should read the references given in *chapter 1.3*. Although a 3D-model can contain more physical aspects, it should not be forgotten that the final code will be very difficult.

### 7.3 Conclusions

A study on the production characteristics of a horizontal well was performed in this report. This was done by developing a 1D-model, which was based on both theoretical and experimental work. The resulting equations were solved by means of efficient and accurate numerical methods, which resulted in a Fortran code. The code was used for a study on all the parameters in the model. Compared to the model of Dikken, several extensions have been made and investigated. Finally, a list with relevant and used literature is given.

The parameter study showed that the pressure drop in the well gives a small increase in the inflow towards the heel of the well. A change in one of the model parameters will result in a change in the pressure drop along the well and therefore also result in a change in the inflow. A higher drawdown at the heel, for example, gives a higher total production rate, but also a higher pressure drop and therefore a less even inflow along the well. Also an increase of the well length gives a less even inflow along the well, in fact the total production rate reaches an asymptotic value if the well is made longer and longer. The inflow can also be influenced by using a variable (small) relative perforated area along the well, this can be obtained by using Inflow Control Devices along the well. The results show that it is possible to obtain an almost even inflow along the well. Although the model contains a lot of the significant physics, some possible extensions, that result in a more accurate model were given.

## Nomenclature

$Q(x)$	=	The volume flux in the well at position $x$ . If $Q > 0$ then the flow goes in the negative $x$ -direction. [ $\text{m}^3/\text{s}$ ]
$q(x)$	=	The inflow in the well at position $x$ . [ $\text{m}^3/\text{s}/\text{m}$ ]
$p_w(x)$	=	The pressure in the well at position $x$ . [Pa]
$p_d$	=	The constant reservoir pressure at a constant boundary [Pa].
$\mathcal{D}_0$	=	The difference in the pressure at the drainage radius and the pressure at the heel of the well [Pa].
$\mathcal{D}_L$	=	The difference in the pressure at the drainage radius and the pressure at the toe of the well. [Pa].
$dp_f(x)$	=	The change in pressure caused by friction. [Pa]
$dp_a(x)$	=	The change in pressure caused by acceleration effects. [Pa]
$f(Q(x))$	=	The friction-factor for the volume flux $ Q $ .
$\alpha$	=	Roughness parameter used in the Blasius frictionfactor for turbulent flow, $\alpha \in [0, 0.25]$ .
$\epsilon$	=	Roughness parameter used in the Haaland friction-factor [m].
$Re = \frac{\rho Q d}{\mu A}$	=	Reynoldsnumber for a pipe.
$\lambda$	=	Experimental factor for the calculation of the correction which is needed because of the inflow in the pipe.
$J_s$	=	The productivity index (PI) per meter or specific PI. The specific PI is a well constant for measuring the performance (= inflow per second) of a well per bar and per meter. Using this parameter makes it possible to compare different wells, with different drawdowns and different lengths. [ $\text{Sm}^3/\text{s}/\text{Pa}/\text{m}$ ]
$d$	=	Inner diameter of the production-pipe. [m]
$A$	=	Inner surface of the production-pipe. [ $\text{m}^2$ ]
$\rho$	=	Density of oil, assumed constant. [ $\text{kg}/\text{m}^3$ ]
$\mu$	=	The viscosity of oil. [ $\text{kg}/(\text{ms}^2)$ ]
$L$	=	Length of the well. [m]
$R_{pa}$	=	Relative perforated area of production line = perforated area/pipe area.
$v_{rad}$	=	The radial velocity in the reservoir. [m/s]
$r_w$	=	The radius of the well. [m]
$r_d$	=	The distance from the constant pressure boundary to the well. [m]
$k$	=	The permeability of the reservoir. [ $\text{m}^2$ ]

## References

- [KA, 1978] : Atkinson, K. E., 1978, ' An Intoduction to Numerical Analysis ',  
*Book*, Wiley.
- [GR, 1984] : Giger, F. M., Reiss, L. H. and Jourdan, A. P., 1984, ' The Reservoir  
Engineering Aspects of Horizontal drilling ', *Article*, SPE 27577,  
presented at the 59th SPE Annual Technical Conference and  
Exhibition held in Houston, Texas, 1984.
- [SJ, 1987] : Joshi, S. D., 1987, ' A Review of Horizontal Well and Drainhole  
Technology', *Article*, SPE 16868, presented at the 62th SPE  
Annual Technical Conference and Exhibition held in Dallas,  
Texas, 1987.
- [SJ, 1988] : Joshi, S. D., 1988, ' Augmentation of Well Productivity With Slant  
and Horizontal Wells', *Article, Journal of Petroleum Technology*,  
june 1988.
- [RD, 1990] : Renard, G. and Dupuy, J. G., 1990, ' Influence of Formation Damage  
on the Flow Efficiency of Horizontal Wells ', *Article* , SPE 19414,  
presented at the SPE Formation Damage Control Symposium held  
in Lafayette, Louisiane, 1990.
- [BD, 1990] : Dikken, B. J., 1990, ' Pressure Drop in Horizontal Wells and its Effect  
on Production Performance ', *Article*, SPE 19824, presented at the  
64th SPE Annual Technical Conferene and Exhibition held in San  
Antonio, 1990.
- [LG, 1991] : Landman, M. J. and Goldthorpe, W. G., 1991, ' Optimization of  
Perforation Distribution for Horizontal Wells ', *Article*, SPE 23005,  
presented at the SPE Asia-Pacific Conference in Perth 1991.
- [KR, 1991] : Korady, V. and Renard, G., 1991, ' Modelling of Pressured Drop for  
Three Phase Flow in Horizontal Wells ', *Article*, presented at the  
6th European IOR-Symposium in Stavanger, 1991.
- [OS, 1992] : Ozkan E., Sarica, C., Hacıislamoglu, M. and Raghavan R., 1992, ' Effect  
of Conductivity on Horizontal Well Pressure Behaviour ', *Article*,  
SPE 24683, presented at the 67th SPE Annual Technical  
Conference and Exhibition held in Washinton DC, 1992.
- [TP, 1993] : Tehrani, D. and Peden, J. M., 1993, ' Critical Reservoir Parameters  
Affecting Succes of Horizontal Wells ', *Article*, presented at the  
European IOR-Symposium in Moscow, 1993.

- [SH, 1993] : Holte, S. T., 1993, ' Pressure Drop in Horizontal Wells - Analytical Approach ', *Internal Report for Norsk Hydro*.
- [BJ, 1993] : Brekke, K., Johansen, T.E. and Olufsen R., 1993, ' A New Modular Approach To Comprehensive Simulation of Horizontal Wells ', *Article*, SPE 26518, presented at the 68th SPE Annual Technical Conference and Exhibition held in Houston, 1993.
- [ML, 1993] : Marett, B. P. and Landman, M. J., 1993, ' Optimal Perforation Design for Horizontal Wells in Reservoirs with Boundaries ', *Article*, SPE 25366, presented at the SPE Asia Pacific Oil and Gas Conference and Exhibition in Singapore, 1993.
- [AH, 1994] : Alvestad, J., Holing, K., Christoffersen, K., Langeland, O. and Stava, O., 1994, *Article*, ' Interactive Modelling of Multiphase Inflow Performance of Horizontal and Highly Deviated Wells ', *Article*, SPE 27577, presented at the 1994 European Petroleum Computer Conference, Aberdeen, 1994.
- [US, 1995] : Utvik, O. H. and Schulkes, R., 1996, *Internal Report for Norsk Hydro*, ' Prediction of pressure drop in Horizontal Wells '.
- [RU, 1996] : Rinde, T. and Utvik, O. H., 1996, *Internal Report for Norsk Hydro*, ' Test of Inflow Control Devices for Horizontal Wells 1996 '.

# Appendix A

## The reservoir

It is assumed that the inflow depends linearly on the pressure difference between the well and a certain constant boundary in the reservoir. It is also, indirectly, assumed that the specific productivity index is constant along the well. This appendix contains the justifications of the linear inflow-drawdown relation and the constant specific productivity index, taking in account the assumptions 5, 7 and 8. In order to be able to give an analytical derivation, it is assumed that the permeability is equal in all the directions. This results in the following reservoir equation, 'Darcy's equation',

$$\mathbf{v}(x, y, z) = \frac{k}{\mu} \nabla p(x, y, z). \quad (\text{A.1})$$

with

- $\mathbf{v}(x, y, z)$  =  $(u, v, w)$ , the velocity of the fluid in the reservoir, [m/s]
- $k$  = the permeability of the reservoir, [m<sup>2</sup>]
- $\mu$  = the viscosity of the fluid, [kg/(ms<sup>2</sup>)]
- $p(x, y, z)$  = the pressure in the reservoir [Pa].

It is assumed that there is a boundary on a constant distance of the well,  $r_d$ , with a constant pressure  $p_d$ . This constant pressure boundary will be used for the derivation of the typical length scale in the reservoir along the flow line in the direction towards the well,  $\Delta l$ .  $\Delta l$  is a measure for the distance on which significant changes in the drawdown occur. For the calculation the following common values are used,  $Q_0 = 2000\text{m}^3\text{7day}$ ,  $L = 1000\text{m}$ ,  $r_w = 0.16\text{m}$ ,  $k = 1\text{Darcy} = 9.8 \cdot 10^{-13}\text{m}^2$ ,  $\mu = 1.3\text{cP}$  and  $\mathcal{D}_0 = 0.3\text{bar}$ . Via the following equation

$$O\left(\frac{Q_0}{L} \frac{1}{2\pi r_w}\right) = O\left(\frac{k \mathcal{D}_0}{\mu \Delta l}\right),$$

it follows that this typical length scale is in the order of one meter, i.e.  $\Delta l = O(1)$ . The constant pressure boundary is assumed to occur on a distance  $r_d$  from the well, the distance  $r_d$  is assumed to be of order  $\Delta l$ . The next typical length scale is for the significant changes in the well pressure in the  $x$ -direction, calculations show that this length is given by  $L$ .

After using the continuity equation for an incompressible fluid,

$$\nabla \cdot \mathbf{v}(x, y, z) = 0,$$

it follows that

$$\left( \frac{\partial^2}{\partial x^2} + \frac{\partial^2}{\partial y^2} + \frac{\partial^2}{\partial z^2} \right) p(x, y, z) = 0.$$

The use of cylindrical coordinates, see Figure A.1, makes it possible to rewrite the equation as

$$\frac{\partial^2 p}{\partial x^2}(x, r) + \frac{1}{r} \frac{\partial}{\partial r} \left[ r \frac{\partial p}{\partial r}(x, r) \right] = 0. \quad (\text{A.2})$$

The derived typical length scales can be used to simplify this equation, the problem will be split into three parts. The first part is that area with  $x < x_{heel}$ , with  $x_{heel} = O(\Delta l)$  in this area the significant changes in both the radial and  $x$ -direction happen on a lengthscale of order  $\Delta l$ . The second and largest part is that area where  $x_{heel} \leq x \leq L - x_{toe}$ , with  $x_{toe} = O(\Delta l)$  holds. In this part of the reservoir, the significant changes in the pressure in the  $x$ -direction happen on a lengthscale of order  $L$ , whereas the significant changes in the pressure in the radial direction happen on a length scale of order  $\Delta l$ . The last part is the section where  $x > L_x$ , for this part holds the same as for the first one. A comparison of the lengthscales gives  $\Delta l \ll L$ , the same yields for the three different mentioned areas. If the two areas at the heel and the toe of the well are assumed to have the same properties as the middle section than the made error is of order  $\Delta l/L$ . So, the significant changes in the pressure in the  $x$ -direction happens now on a lengthscale with length  $O(L)$ , whereas all the significant changes in the radial direction occur on a lengthscale of order  $\Delta l$ .

The variables in eq. (A.2) can now be scaled as,  $x = x' \cdot L$  and  $r = r' \cdot \Delta l$ . This results in the following differential equation:

$$\frac{\Delta l^2}{L^2} \frac{\partial^2 p}{\partial x'^2}(x', r') \frac{1}{r'} \frac{\partial}{\partial r'} \left[ r' \frac{\partial p}{\partial r'}(x', r') \right] = 0.$$

After ignoring the  $O(\Delta l^2/L^2)$ -terms, the following equation remains

$$\frac{1}{r'} \frac{\partial}{\partial r'} \left[ r' \frac{\partial p}{\partial r'}(x', r') \right] = 0,$$

with boundary conditions,  $p(x', r_w \Delta l) = p_w(x' \cdot L)$  and  $p(x', r_d \Delta l) = p_d$  and general solution

$$p(x, r) = a(x) + b(x) \log(r).$$

It should be noted that the boundary of the problem is given by  $r = r_w$  and  $r = r_d$ , since the changes in the gradient of the pressure in the  $x$ -direction are ignored. All this results in the unscaled pressure distribution in the reservoir

$$p(x, r) = p_w(x) - [p_d - p_w(x)] \frac{\log\left(\frac{r}{r_w}\right)}{\log\left(\frac{r_d}{r_w}\right)} \quad (\text{A.3})$$

Via eq. (A.1) it follows that the radial velocity,  $v_{rad}(x, r)$ , is given by

$$v_{rad}(x, r) = \frac{k}{\mu} \frac{\partial}{\partial r} p(x, r). \quad (\text{A.4})$$

If the pressure drop due to the pipe wall is negligible compared to the pressure drop in the reservoir, then equation (A.4) combined with eq. (A.3) and the inflow-drawdown equation,

$$q(x) = 2\pi r_w v_{rad}(x, r_w),$$

result in the linear inflow-drawdown equation

$$q(x) = J_s [p_d - p_w(x)]$$

with the constant specific PI;

$$J_s = \frac{2k\pi}{\mu} \frac{1}{\log\left(\frac{r_d}{r_w}\right)}. \quad (\text{A.5})$$

## Appendix B

### The pressure drop in a pipe with radial inflow

The pressure drop in a pipe with a constant volume flux  $Q$ , a length  $\Delta x$  and a complete developed turbulent regime is given by

$$\Delta p_{fric,Q} = \Delta x \frac{\rho}{A^2} \frac{f(Q)}{2d} Q^2, \quad (\text{B.1})$$

with

- $\Delta p$  = The total pressure loss in the pipe [Pa].
- $\Delta x$  = The length of the pipe [m].
- $f(Q)$  = Friction factor for a completely developed turbulent pipe flow.

For the description of the pressure drop in a pipe with a non-constant volume flux, equation (B.1) is not valid anymore due to several reasons and should be modified. First of all, the inflow increases the volume flux in the well, which results in the pressure loss due to the accelerational effects, see section 2.2. The accelerational pressure drop can be determined analytically and gives therefore no problems. The main problems are caused by the changes in the friction. It was assumed that the well flow was fully developed, but probably the flow will be developing along the whole well. The inflow results in extra internal friction due to the higher velocity differences in the well, but the inflow results gives also a decrease of the inflow due to a lubrication effect. The changes in pressure drop are partly taken in account via the acceleration term, but the changes in the friction are not. The changes in the friction due to the inflow can be contracted in a so-called correction term, which has to be determined via experiments.

All the experiments on the correction term, see [US, 1996], are done with a perforated pipe with a certain length,  $\Delta x$ , of a few meters. The pressure drop along such a pipe,  $\Delta p$  is given by

$$\Delta p = \Delta p_f + \Delta p_a + \Delta p_c,$$

with

- $\Delta p_f$  = the pressure drop due to friction, described by eq. (B.1) where the volume flux at the beginning of the test section is used, i.e. the lowest volume flux, and assumed to be constant [Pa],  
 $\Delta p_a$  = Integrated version of eq. (2.9) [Pa],  
 $\Delta p_c$  = The change in the friction due to the inflow [Pa].

It should be noted that the use of eq. (B.1) gives another result than the integrated version of (2.4). But via some integration rules one can find that the introduced error is of order  $O(q(x)/Q(x))$ . The pressure difference between the two endpoints of the test section is measured,  $\Delta p_{meas}$  and this gives the following equation for  $\Delta p_c$

$$\Delta p_c = \Delta p_{meas} - \Delta p_f - \Delta p_a.$$

Since, the obtained experimental data contain a lot of noise, some scaling of  $\Delta p_c$  is useful. The typical pressure scale in the obtained measurements is the value of  $\Delta p_f$  this results in the following formula

$$\Delta p_c = \kappa \Delta p_f.$$

Some more typical scales exist. The inflow can be compared with the radial volume flux at each position;  $\kappa = \tau q(x)/Q(x)$ . Experiments show that if the total inflow along the test section is small compared to the volume flux at the start of the test section, the inflow makes the pressure drop less. This is caused by a so-called lubrication effect; the axial flow experiences a more smooth pipe wall. This results in the final typical scale of the experiments. The inflow gives a lubrication effect which depends on the velocity of the inflow,  $\sim O(d)$ . The inflow also gives velocity differences in the axial flow and therefore additional fluid friction. This friction effect is the strongest in the neighbourhood of the pipe wall, therefore the friction effect is of order  $O(d)$ . The final result is the following formula for the correction term

$$\Delta p_c = -\lambda d \frac{q(x)}{Q(x)} \Delta p_f.$$

Experiments with different pipes with different diameters show that the maximal difference in  $\lambda$  is about 25% of its average value,  $\lambda = 25$ . This can be considered as an acceptable error, in particular when one knows that the integration error for the friction,  $\sim O(q(x)/Q(x))$  does not depend on the pipe diameter and introduces in this way an additional (small) error.

What remains now is the pressure gradient of the correction term. If the length of the pipe section is small compared to a well length then the values of  $q(x)$  and  $Q(x)$  can assumed to be constant. This results in the following equation

$$\frac{dp_c}{dx} = -\lambda d \frac{q(x)}{Q(x)} \frac{dp_f}{dx}$$

# Appendix C

## Stability

This appendix contains the conditions which lead to a stable solution of the model described in chapter 2 when it is solved by means of the numerical methods described in chapter 3. There exist several definitions for the stability, in this report the following one will be used:

*Definition C.1:* A solution  $Q^{(M)}$  is called stable if there exists a constant  $C$ , independent of  $n$ ,  $Q^{(0)}$  and a nearby solution  $\hat{Q}^{(0)}$ , so that

$$\|Q^{(n)} - \hat{Q}^{(n)}\| < C \|Q^{(0)} - \hat{Q}^{(0)}\|, \quad \forall 1 < n < M,$$

holds for all  $1 < M < \infty$ .

Since the number  $M$  equals the number of iterations and since the number of iterations will always be bounded, it follows via an induction argument and Definition C.1 that  $Q^{(M)}$  can be called a stable solution if the following holds

$$\|Q^{(n+1)} - \hat{Q}^{(n+1)}\| < C_{(n)} \|Q^{(n)} - \hat{Q}^{(n)}\|, \quad \forall 1 < n < \infty, \quad (C.1)$$

for all nearby initial guesses  $\hat{Q}^{(0)}$ . Suppose that the solutions  $Q^{(n+1)}$  and  $\hat{Q}^{(n+1)}$  are obtained via,  $Q^{(n+1)} = A^{(n)-1} r^{(n)}$  and  $\hat{Q}^{(n+1)} = \hat{A}^{(n)-1} \hat{r}^{(n)}$ , see eq. (3.12), then it follows that the condition (C.1) is equivalent with:

$$\|A^{(n)-1} r^{(n)} - \hat{A}^{(n)-1} \hat{r}^{(n)}\| < C_{(n)} \|Q^{(n)} - \hat{Q}^{(n)}\|, \quad \forall 1 < n < \infty.$$

This condition can be achieved by demanding non-singular matrices  $A^{(n)-1}$  and  $\hat{A}^{(n)-1}$  and bounded right hand side vectors  $r^{(n)}$  and  $\hat{r}^{(n)}$  during all the iterations steps. In order to keep things simple a continuity argument is used, which means that the final desired properties for  $Q^{(0)}$  are assumed also to hold for  $\hat{Q}^{(0)}$ . All this will result in a stable solution  $Q^{(M)} \forall 1 < M < \infty$ .

First the conditions for a non-singular matrix  $A^{(n)}$  will be derived, therefore, the following definitions and theorem will be used.

**Definition C.2:** A matrix  $A$ , of order  $K > 1$ , is called weakly diagonally dominant if  $|a_{ii}| \geq \sum_{i=1, i \neq j}^K |a_{ij}|$  and for at least one value of  $i$  yields the '>'-sign.

**Definition C.3:** A matrix  $A$ , of order  $K > 1$ , is irreducible if and only if for every choice of  $i$  and  $j$  with  $1 \leq i, j \leq K$  and  $i \neq j$  yields that either  $A_{ij} \neq 0$  or  $(\exists k_1, k_2, \dots, k_p)$  such that  $a_{ik_1} a_{k_1 k_2} \dots a_{k_p j} \neq 0$ .

**Theorem C.1:** An irreducible and weak diagonal dominant matrix with bounded coefficients is non-singular.

The condition for a weak diagonal dominant  $A^{(n)}$  can be made a bit stronger for the inner nodes. This results in:

$$|d_i^{(n)}| > |l_i^{(n)}| + |u_i^{(n)}|, \quad \forall i = 1, \dots, N-1.$$

After ignoring the  $O(1)$ -terms one can find the following conditions for all the inner nodes:

$$0 < h < \frac{2A^2}{J_s \rho |Q_i^{(n)}|}, \quad \forall i = 1, \dots, N-1, \quad (\text{C.2})$$

and

$$|Q_{i+1}^{(n)}| \neq |Q_{i-1}^{(n)}|, \quad \forall i = 1, \dots, N-1. \quad (\text{C.3})$$

If one takes a look at the boundary coefficients in section 3.2, than it can be concluded that the boundary coefficients do not give any problems. What remains now are the conditions which make the tridiagonal matrix  $A^{(n)}$  irreducible. It can be calculated that  $A^{(n)}$  is irreducible if and only if

$$l_i^{(n)}, d_i^{(n)}, r_i^{(n)} \neq 0, \quad 1 < n < M,$$

holds for all the the "existing" matrix coefficients. This can be obtained for all the matrix coefficients by eq. (C.2). Concluded, a monotonic  $Q^{(n)}$  and a mesh width that satisfies

$$0 < h < \frac{2A^2}{J_s \rho |Q_i^{(n)}|}, \quad \forall i = 0, \dots, N. \quad (\text{C.4})$$

results in a non-singular  $A^{(n)}$ .

The matrix  $A^{(n)}$  has to be non-singular for all  $n > 1$ , i.e. the conditions for a non-singular  $A^{(n)}$  have to hold also for all  $n$ . It is not so difficult to verify that if the mesh width is small enough and if  $Q^{(n)}$  is monotonic that the next iterate  $Q^{(n+1)}$  will be monotonic again. The only remaining problem is now to start with a mesh width that is small enough during all the iterations. For this calculation it is assumed that the production rate at the toe is the largest production rate along the well,  $Q_0^{(n)}$  will therefore be used for the calculation of the maximum allowed mesh width. If the following common values

are used,  $d = 0.16\text{m}$ ,  $\rho = 781,0\text{kg/m}^3$ ,  $J_s = 10\text{Sm}^3/\text{day}/\text{bar}/\text{m}$  and  $Q_0^{(n)} = 2000\text{m}^3/\text{day}$  then the maximum allowed mesh width appears:

$$h < 4.0 \cdot 10^4 \text{m}.$$

Although this is a very large allowed mesh width, it should not be forgotten that the ignored  $O(1)$ -terms might have a certain influence on the stability, i.e. the diagonal dominance.

It was also mentioned that the coefficients in the matrix and the right hand side vector have to remain bounded during the iteration process. This is not so difficult, only the computed version of the derivative of the friction term can give some problems. But for a inner node, this term can be written as:

$$\frac{\hat{f}(Q_{i+1}^{(n)}) - \hat{f}(Q_{i-1}^{(n)})}{Q_{i+1}^{(n)} - Q_{i-1}^{(n)}} = 2 \frac{d\hat{f}(Q_i^{(n)})}{dQ} - \frac{1}{3} (Q_{i+1}^{(n)} - Q_{i-1}^{(n)})^2 \frac{d^3\hat{f}(\tilde{Q})}{dQ^3}, \quad Q_{i+1}^{(n)} < \tilde{Q} < Q_{i-1}^{(n)}.$$

The Haaland equation for the friction factor has the properties that its third derivative remains bounded as long as  $Q_i^{(n)} < \infty$ . In case of a Neumann boundary condition a similar result can be found.

# Supplement I

## Norsk Hydro

Norsk Hydro is established in 1905 to utilize Norway's large resources of hydro electric power in the first industrial manufacture of nitrogen-based mineral fertilizer. Nowadays, Norsk Hydro is the world leading manufacturer of mineral fertilizer. Energy, both in the form of hydro electric power and petroleum, has been the basis for Hydro's growth and represents an important connection between the different business areas. In 1951 the company expanded its activities by starting to manufacture magnesium. In 1967 this energy-intensive light metal activity was extended to include aluminium productivity. Today the company ranks among the world's leading manufacturers in both aluminium and magnesium. When exploration for oil and gas was started in the North Sea, Hydro participated right from the beginning when the first licenses were granted on the Norwegian shelf in 1965. Hydro and its partners found oil and gas in the Ekofisk field in 1971. These finds formed the basis for the company's development as an important producer of oil and gas. As operator for large offshore projects, amongst others the Oseberg field in the North Sea, Hydro has established itself as a fully fledged oil company. Oil production in the North Sea gave Hydro long-term access to natural gas liquids which has provided the basis for further expansion into the petrochemical industry. Hydro now has refinery operations and retail marketing companies for petroleum products in Norway, Sweden and Denmark.

Most of the Hydro's involvement in the oil and gas business is connected with activities on the Norwegian shelf. Hydro has participated in two-thirds of all drilling on the Norwegian shelf and is one of the leading oil companies operating in Norway. Hydro has interests in several of the largest oil and gas fields on the continental shelf, including Gullflaks, Ekofisk and Frigg. In addition, the company is operator for development projects such as Troll Oil. Hydro is joint owner of the Swedish refinery Scanraff and markets petrol and petroleum products through its own petrol stations and distribution network in Norway, Sweden and Denmark. Some data about the company.

Employees world wide	:	35.000 people
Employees in Norway	:	17.000 people
Turn over	:	80.000 million Nok
Profit	:	2.800 million Nok

# Supplement II

## Experimental Work

Mostly, the produced oil contains water and also gas. This gives a multiphase axial flow in both the production pipe and transport pipe and also a multiphase radial inflow into the production pipe. The water and, in particular, the gas can have a significant influence on the pressure drop in the different pipe sections. The pressure drop in the well and production pipe, depends on the gas-oil ratio (GOR) and the water-oil ratio (WOR). Since it is very hard to calculate the pressure drop of a multiphase system, some experiments have been performed in order to get the needed insight and correlations.

The experiments were performed at a low pressure loop with a perforated pipe. This system offers the possibility for air and water phases in both the axial and radial direction, where the radial inflow is uniformly divided along the test section. This system loop is not used for tests with oil phases, those tests are performed with a closed high pressure rig. The different performed experiments with the low pressure rig were divided in different sets, the first set was done with only axial water flow. This set is necessary for determining the roughness of the pipe. Using the obtained data for several values of the volume flux, range  $10\text{m}^3/\text{hour}$  until  $120\text{m}^3/\text{hour}$ , in combination with eq. (2.4) gives an estimation of the roughness parameter. This test set can also be used for comparison with the following sets of experiments. The second set of experiments was done with only water in both the axial and radial direction. This set had several goals; obtain more data, compare with previous data and compare with the following set. For the axial flow a few values were used and for each of these values a sequence of values for the radial inflow was used (range  $0\text{m}^3/\text{hour}$  until  $20\text{m}^3/\text{hour}$ ). The obtained test matrix was used with the obtained roughness parameter and the formula given by equation (2.5). The last performed test set was a multiphase one, the used water in all directions did contain a percentage of air, 0% until 5%. Using different percentages of the air in the water and using the combinations as used in the second set gives a three dimensional test matrix.

The main goal of the experiments is to obtain correlations between the GOR, the WOR and the pressure drop in the well. Therefore the pressure, i.e. the pressure difference with the absolute atmospheric pressure, was measured at four different positions along the test loop. A pressure meter, accuracy 5Pa, was placed at the beginning and at the end of the test section, whereas the two others were placed at approximately

one-third and two-third of the test length. During the experiments of each 2-3 minutes the pressure was measured each 10 seconds. By dividing the pressure difference between two meters by their distance the pressure drop can be obtained. It should be noted that the pressure drop given by the pressure difference between the first and the last gives the most accurate information since the division is done with the longest possible length.

The obtained data were analysed with some statistical tools. Due to several reasons there was some noise present. One can think about temperature, fluctuations in the main flux and pressure differences in the atmospheric pressure. But since there were a lot of measurements, and since the length of the test loop is about 15m, one can say that the influence of the noise has not any major influence on the measurements. The obtained data of the first set show that, inherent to the expectations, the pressure drop increases if the main, axial, flow increases and, more suprisingly, that the roughness parameter could depend on the main flux. The measurements in the second set show a know fact. For fixed axial flow, increasing radial inflow gives at first a small decrease of the pressure drop and after a certain value of the axial flow-radial flow ratio a small increase in the pressure drop. The complicated last set gives a lot possible correlations and reactions. The main result is that for each fixed pair of axial and radial flow, a increase of the air percentage gives an increase of the pressure drop.

The data from the experiments behave like expected. In particular the first and second set give approximately the same results as the ones calculated by eq. (2.8) respectively eq. (2.5). Since there are not so many accurate relations for the last set, the obtained data are very useful. The data show the same trend as the known formulas, but the data can help to gain the better insight and correlations. Therefore the whole project can be seen as succesfull.